# SILO DESIGN, ANALYSIS AND OPTIMIZATION OF ITS COMPONENTS

**By**

**Parth Parekh**

**14MMED09**

NIRMA UNIVERSITY
INSTITUTE OF TECHNOLOGY
NAAC ACCREDITED 'A' GRADE

DEPARTMENT OF MECHANICAL ENGINEERING
INSTITUTE OF TECHNOLOGY
NIRMA UNIVERSITY
AHMEDABAD-382481
MAY 2016

# SILO DESIGN, ANALYSIS AND OPTIMIZATION OF ITS COMPONENTS

Major Project Report

Submitted in partial fulfillment of the requirements

for the Degree of

Master of Technology in Mechanical Engineering (Design Engineering)


Submitted By

Parth Parekh

(14MMED09)

Guided By

Dr. Mitesh B. Panchal


NIRMA UNIVERSITY
INSTITUTE OF TECHNOLOGY
NAAC ACCREDITED 'A' GRADE


DEPARTMENT OF MECHANICAL ENGINEERING
INSTITUTE OF TECHNOLOGY
NIRMA UNIVERSITY
AHMEDABAD-382 481

MAY 2016

# Declaration

This is to certify that

1. The thesis comprises of my original work towards the degree of Master of Technology in Mechanical Engineering (Design Engineering) at Nirma University and has not been submitted elsewhere for a degree.

2. Due acknowledgment has been made in the text to all other material used.

Parth Parekh

14MMED09

## Undertaking for Originality of the Work

I, Parth Parekh, Roll. No. 14MMED09, give undertaking that the Major Project entitled "SILO DESIGN, ANALYSIS AND OPTIMIZATION OF ITS COMPONENTS" submitted by me, towards the partial fulfillment of the requirements for the degree of Master of Technology in Mechanical Engineering (Design Engineering) of Nirma University, Ahmadabad, is the original work carried out by me and I give assurance that no attempt of plagiarism has been made. I understand that in event of any similarity found subsequently with any published work or any dissertation work elsewhere; it will result in severe disciplinary action.

___________________________

Signature of Student

**Date:** ___________________

**Place:** Nirma University,Ahmadabad

**Endorsed By**

( Signature of Institute Guide)

# Certificate

This is certify that the Major Project Report entitled “Silo Design, Analysis And Optimization Of Its Components ” submitted by Mr. Parth R. Parekh(14MMED09), towards the partially fulfillment of the requirements for the awards of Degree of Master of Technology in Mechanical Engineering (Design Engineering) of Institute of Technology, Nirma University, Ahmedabad is record of work carried out by him under our supervision and guidance. In our opinion, the submitted work has reached a level required for being accepted for examination. The result embodied in this major project, to the best of our knowledge, has not been submitted to any other University or Institute for award of any degree..

Dr. Mitesh B. Panchal
Department of Mechanical Engineering,
Institute of Technology,
Nirma University,
Ahmedabad-382481.

Dr. R. N. Patel
Professor and Head,
Department of Mechanical Engineering,
Institute of Technology,
Nirma University,Ahmedabad-382481.

Dr. P N Tekwani
Director
Institute of Technology,
Nirma University,
Ahmedabad-382481

# Acknowledgments

I would like to show my gratitude to those who give me opportunity to work in organization and support me directly or indirectly for completing entire dissertation and provide me valuable guidance throughout project duration.

First of all, I would like to thank my internal project guide Dr. Mitesh B. Panchal for that support throughout this project and give me valuable guidance from there busy schedule. Also I would like to thanks to my external guide Mr. Kamlesh Patel for provide me opportunity, facility, and support from there staff member and give me opportunity for live project and give me adequate information regards to project.

I would like to thanks Head of Department Dr.R.N.Patel and other faculty of Mechanical Department for helping me for dissertation work.

I would also like to thank Dr R N Patel, Head of Mechanical Engineering Dept. and Director Dr. P N Tekwani for providing opportunity to work on this problem and also to the management of Nirma Education and Research Foundation (NERF) for providing excellent infrastructure and facilities whenever and wherever required.

I would also like to thank god, my parents and all my friends who have help me and for the moral support throughout the dissertation. I remain highly grateful to them and it is my earnest desire to acknowledge all of them.

**Parth R Parekh**

# Abstract

Silos and hoppers are widely used in a many different industries for storing a huge range of different solids. The value of these tanks to society exceeds by far the economic value of the tanks and their contents. This is because the failure of tanks and their accessories is not limited to the immediate danger to nearby human lives, but also to a large extent leads to serious consequences and very likely to long-term environmental damages. The sizes of these silos may vary from capacities less that 1 tonne to the largest containing as much as 100 000 tonnes. So, the Design of the silo should be done properly. This thesis contains designing of the silo as per various applicable code and standards. The silo is designed for various types of load acting on it e.g. dead load, live load, wind or seismic load, load during filling and discharging of bulk material etc. Stress calculation has been done for Silo having storage capacity of 115 $m^3$ for storing plastic pellets. This include different kind of stresses developed in silo i.e circumferential stress as 5.10, axial stress, equivalents stresses. Finally all stresses are verified by allowable stress values of construction material according to standards such as 39.1 and then it is verified by using FEA analysis. Critical phase in silo is transition phase where cylindrical shell meets conical hopper which is vulnerable so that proper design of supporting ring girder which can prevent the failure.

# Contents

# List of Figures

# List of Tables

# Nomenclature

| Variables | Physical Quantity |
|---|---|
| d | Inner diameter of the silo |
| r | Inner radius of silo |
| $d_a$ | Lower diameter of cone |
| $\lambda_f$ | Pressure ratio during filling |
| $\lambda_e$ | Pressure ratio during emptying |
| $\phi$ | Horizontal pressures on the wall |
| $P_h$ | Wall friction pressures on the wall |
| $P_w$ | .Vertical pressures on the wall |
| $P_v$ | Density of stored material |
| W | Perimeter |
| U | Mean hydraulic radius |
| R | Design Length |
| $\delta_f$ | Angle of wall friction during filling |
| $\delta_e$ | Angle of wall friction while emptying |
| $\mu_f$ | Coefficient of wall friction while filling |
| $\mu_e$ | Coefficient of wall friction while emptying |
| $\theta$ | Angle of inclination of hopper wall |
| E | Welding joint efficiency |
| $Pi(z)$ | Variation of pressure along bin depth |
| Z | Depth of silo in meter |
| G | Dead Weight of Silo |
| $\rho$ | Density of construction material |

| | |
|---|---|
| $V_b$ | Basic Wind Speed |
| $V_z$ | Wind Speed at specic depth z |
| $k_l$ | Probability factor ( risk coecient ) |
| $k_2$ | Terrain, height and structure size factor |
| $k_3$ | Topography factor. |
| $\sigma_{phi}$ | Circumferential Stress |
| $\sigma_{x,g}$ | Axial Stress due to dead load |
| $\sigma_{x,z}$ | Axial stress due to additional dead load |
| $\sigma_{x,p}$ | Axial Stress due to roof load |
| $\sigma_{x,w}$ | Axial Stress due to wind load |
| $n_z$ | Load due to pressure per meter |
| $P_{he}$ | Pressure during Discharging |
| $P_{hf}$ | Pressure during Filling |
| $P_o$ | Design Over pressure |
| $n_{phi}$ | Circumferential load per meter |
| $P_z$ | Design wind pressure at depth z |
| $A_p$ | Projected area for wind |
| $M_{wio}$ | Wind moment due to wind load Hwi |
| $H_{wi}$ | Wind load on projected area |

# Chapter 1

# Introduction

Silo may be classified as storage structure generally used for storing coal, cement, food grains, and other granular materials. Steel silos may be directly supported at ground level in which case walls are extend to the foundation and the stored material rest either on the foundation or directly on the ground. As an alternate the stored material may be supported by silo bottoms elevated above the ground. Elevated steel silos may be supported by columns directly attached to the shell or by special supporting steel or concrete structural framing. In case of small diameter silos, the metal walls may extend down to the foundation and support the entire structure.

## 1.1 Components of Silo

The Figure 1.1 shows different components of Silo.

1) Conical bottom,

2) Cylindrical bin,

3) Hemispherical roof, and

4) Supports

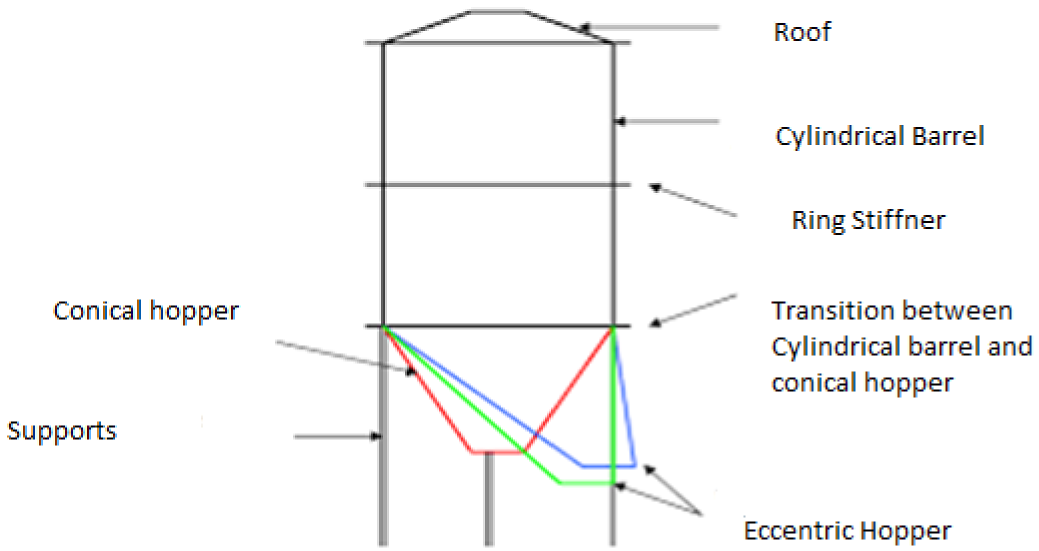


Figure 1.1: Silo components

## 1.2 Classification

Silos are classified based on following points.

- Bin size and geometry
- Type of flow
- Structural material of wall

### Size and geometry of bin

The size and geometry of bin depend on the functional requirements such as the storage volume, the method, rate of discharge, properties of the material which is stored, space available and economic considerations. Bins are usually consist of a vertical sided section with a flat bottom or a bottom which have inclined sides, which is known as the hopper. They are usually square, circular or rectangular in c/s and may be arranged in groups or singly. Circular bin structures are more efficient structures than rectangular or square bins structures, leading to lower the material cost. For the same height, a square bin structures provides more storage space than a circular bin structures whose diameter equals the length of the side of the square bin structure. Flat- bottom bins structures require lesser height for a given volume of stored material. The bin size is determined by discharge rates, feeding and the maximum quantity of material to be stored. High discharge rate requires deep hoppers with steep wall. Flat bottomed bin usually has low discharge rate and is used when the time of storage is long, the discharge is infrequent and the volume of storage is high.

### Type of Flow

There are two types of flow as shown in Figure 1.2.

- Mass flow
- Funnel Flow

Discharge pressure is affected by pattern of the flow and so the flow assessment must be done before calculation of loads from the stored material. The flow type depends on the coefficient of wall friction and the inclination of the hopper walls. Funnel flow occurs in squat bins with shallow hopper walls whereas mass flow occurs in deep bins with steep hopper walls.

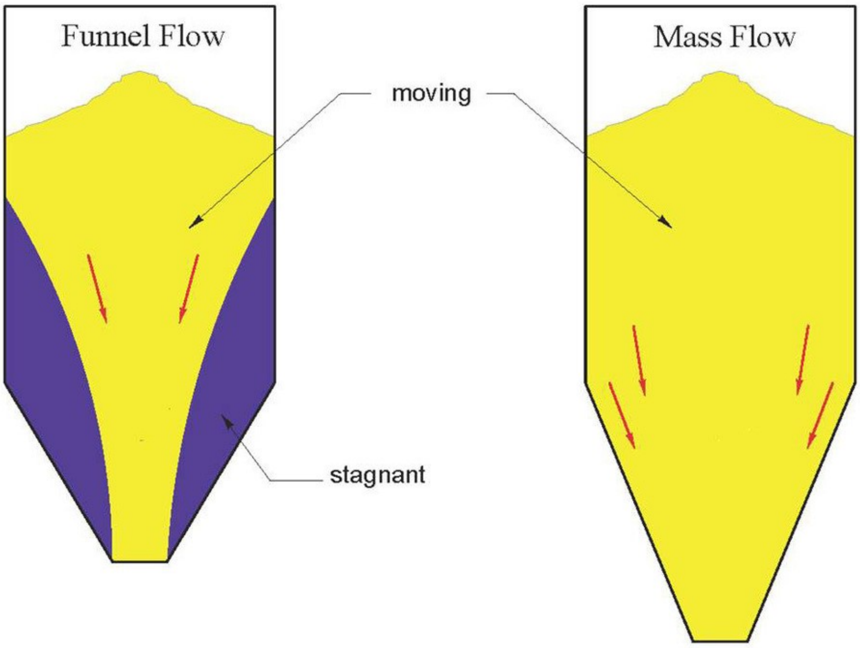


Figure 1.2: Type of flow in silo

## Structural material of the wall

Most of bins are constructed from reinforced concrete or steel. The economic choice depends upon the material costs as well as the costs of fabrication, erection. Other factors such as available space also influence the selection. The main advantage of aluminum bin is resistant to corrosion. The metal wall may be require lining to prevent excessive wear, and the metal walls are prone to condensation which may damage stored products such as sugar, granular, grain , etc. which are moisture sensitive. Metal bins, usually carry the lateral forces by hoop tension. They are more prone to failure by buckling under excessive vertical forces.

Silo can be further classified as below and as shown in Figure 1.3 & Figure 1.4:

1. As per material being used
   - Concrete silo
   - Metal silo
2. As per shape of the circular bin
   - Circular
   - Square or Rectangular
3. As per shapes of the bottom
   - Hopper bottom (cone /pyramid)
   - Flat bottom
4. As per eccentricity of the bottom.
   - Concentric silo
   - Eccentric silo

Figure 1.3: Circular silo

Figure 1.4: Eccentric and concentric silo

# Chapter 2

# Literature review

This Chapter comprises of the literature survey for the project work. Literature survey mainly includes, pressures calculation, stored material, construction procedure, interaction between grains and walls of its storage structure, different structure of silo bottom and pressure distributions, design and analysis and optimization of the silos.

## 2.1 2.1 Review of published papers.

P.Vidal. et al[1] proposed 3D finite element analysis for the filling of cylindrical silos having an eccentric hopper, by using different boundary conditions to silos supported on discrete columns or the transition. The analysis included the options of the presence or absence of reinforcement in the walls and transition. The results for the pressures on the wall for a flexible wall and all the boundary conditions were compared with those for a silo with a rigid wall. The membrane stresses and meridional and circumferential bending moments were then evaluated in the silo wall and in the reinforcing elements. The influence of the eccentricity of the hopper a silo of intermediate eccentricity was analyzed, and conclusions were drawn for the optimal design of these structures.

D. Briassoulis [2] have done the analysis of the behavior and the state of stress developing in a silo shell under real asymmetric pressure distributions concerning both storing and discharge. The results obtained suggest that the design of such structures may not neglect the asymmetric features of the real pressures developed by the stored material.

Y. Zhao,J.G.Teng[3] Generally cone cylinder-skirt transition junction is subject to a large circumferential compressive force which is derived from the horizontal component of the meridonal tension in the conical hopper, so either a ring is provided or the shell walls are locally thickened to strengthen the junction. Extensive theoretical studies have examined by Y.Zhao and J.G.Teng for the buckling and collapse strengths of these junctions, leading to theoretically based design proposals. They presents the results of a series of tests on cone-cylinder and skirt-ring junctions in silo under simulated bulk solid material loading. In addition with the test results including geometric imperfections and failure behavior, the determination of buckling modes and loads based on displacement measurements is done in detail. Silos are used in food industries to store different types of food, dairy, cement, petroleum and agricultural products. Shell structure design is critical under the external load.

PAP AYUGA [4] has investigated the structural effects of the patch load. A 3D FEM model has been developed to model cylindrical flat bottom silos made of corrugated walls. Firs, silos were modeled only with the effect of the symmetrical pressure distribution. The structural effects at this stage were compared to those obtained in a further stage, where the patch-load was introduced in the model. The purpose of his research work was to understand the structural effects of the (see figure 8. l)patch-load as described in the Euro code, as well as validate analytical expressions to determine these effects more easily.

Fuat Tinis.et al [5] proposed that cylindrical silo walls are subjected to both normal pressures and vertical friction shear or traction due to stored material inside the silo which vary along the wall. The normal pressure on cylindrical walls cause circumferential stress and the vertical frictional shear will cause cumulative axial compressive stress. Due to complexity of the problem, the numerical integration techniques and finite element are very widely used for collapse and buckling analysis.

Juana, et al [6] presented different 3D models whose distinguishing feature is the simulation of both stored material and silo walls, without resorting to simplifications. The models developed predict the stress state of cylindrical metal silos flat bottomed, subjected to the action of stored granular material in their interior. The behavior assigned to the stored material is elastic, and that assigned to the structure is the classical bi linear elastic-perfectly plastic, typical of metallic materials such as steel. Two geometric parameters are analyzed: thickness of the wall and height. The results obtained from numerical methods (hoop, vertical, normal, shear stresses) are compared with those obtained with ENV1993-1-6.

Dr.John W.Carson [7] Silos and bins fail with a frequency which is higher than almost any other industrial equipment. Sometimes the failure only involves distortion or deformation which while unsightly does not pose safety or operational hazards. In other case failure involves complete collapse of the structure with accompanying loss of use of life. The major causes of silo failures are due to shortcomings in one or more three categories.

George G. Chase [8] has done pressure calculation as per the janssene equation which is acting on the silo wall and has done calculation for the outlet of cone and cone angle for conical hopper design.

C.Y. Song. [9] investigated the structural behavior of circular steel silos subject to patch loads. The investigations shows that the patch loads have a great effect on the stress states in the silo from the linear elastic analysis (LA). Geometrical non linearity and primary pressures have beneficial effect. Fourier decomposition of the two square-shaped patch loads show that the effect of the shape of patch loads depends not only on the harmonic index, but also on particular stress component. For a pressure with a lower harmonic index (e.g. cos h, cos 2h), only limited effect was observed for all stress components. A pressure with medium-sized harmonic index (cos 4h, cos 6h) has a great effect on meridional compressive stress, while for higher harmonic index; the effect was significant for von Mises equivalent stress. Buckling analysis with geometrical non-linearity and material non-linearity taken into account show that the effect of patch loads could be covered by a certain percentage increase of the vertical frictions, if the patch load approach were adequate to represent the non-uniformity of wall pressures in circular flat bottomed steel silos.

Adam J. Sadowski1 and J. Michael Rotter F.ASCE [10] has done significant work for eccentric discharge. The most critical loading condition for slender thin-walled metal silos has long been recognized to be the condition of discharge, with eccentric discharge causing catastrophic failures than any other. Two key reasons for this high failure rate are the difficulties in characterizing the pressure distribution caused by eccentric solid flow, and in understanding the associated unsymmetrical stresses in the silo wall. Some studies have addressed eccentric discharge analysis and linear elastic behavior. In his study, the eccentric discharge pressure is characterized using the new rules of the .European Standard EN 1991-4 on Silos and Tanks.

This description of unsymmetrical pressures permits a study of the structural behavior leading to buckling during eccentric discharge, including the critical effects of sensitivity of imperfection and change of geometry, to be undertaken using geometrically and materially nonlinear computational analyses. The mechanics of the behavior is found to be quite complicated. A silo which is safe under axisymmetric loading is found to be susceptible to catastrophic stability failure under eccentric discharge.

# Chapter 3

# Load consideration

There are several types of the load which may appear on the silo while in operation or in idol condition as well which are described in the(see figure 8. l) detail below.

## 3.1 Equipment Load

The principle loads for silo design are due to stored material and forces from other sources including; equipment load, dead load, wind load, roof and floor live loads, forces, seismic loads applied at restrain of attached items. Equipment may apply major live load on the structure. First, equipment manufacture should be able to predict the load which their equipment will imposed but if this equipment are vibrating it may bring out changes in other loads. For example the material which is stored may become compacted acquiring higher density and change flow characteristic with final change in lateral and vertical load. Belt conveyor and their support components can bring large live and dead load. It is recommended that fixed or pinned connection of conveyor support to a silo roof not be permitted.

## 3.2 Wind Load

Silo structure should be designed to resist the effects of overturning caused by earthquake forces or wind. Earthquake load and wind load should not be assumed to act simultaneously. Whichever is the more will be taken in design. Practically all codes permit an increase of soil bearing values and allowable stress when either wind or earthquake acts alone or in combination with the dead load and live load. Wind load for silo can be in any lateral direction and generally should be considered as negative on lee ward side and positive pressure on the wind ward side.

## 3.3 Sesmic Load

Earthquake load may affect both stability and strength of silo and bunker. Walls and columns supporting silos and bunkers may be particularly vulnerable to earthquake forces. In the absence of better code requirement on seismic design of silo to resist lateral load different approach is given by IS 1893 (part 1) on silo and bunker. The suggested approach is based on the following assumption

1. Only a fraction of the stored material weight need to be considered when computing seismic forces. For simplicity the seismic forces on the fraction is treated as lateral static force applied at the centroid of the entire stored mass and acting in any horizontal direction. Generally 80 percent of the weight of the stored material is consider as an effective weight,

2. Seismic forces can act in any horizontal direction. Vertical seismic force is neglected for most aspect of seismic design.

3. The weight of the stored material in a suspended hopper should not be reduced to an effective weight value.

4. When silo bottom are on support that are independent of the silo walls these two independent structures will share the lateral force from seismic action on the effective weight.

## 3.4 Dead Load

It includes weight of silo, ring beam, roof, self- walls, hopper - plus the weight of item supported by the silo. These loads outside and inside service platform, equipment on silo roof overhead gallery etc. Many of these loads can only be estimated in the early phase of design. Dead load of silo bottom that rest on independent support should be separated from those affecting the silo walls.

## 3.5 External Loads

A silo is a flexible membrane. The walls of an isolated circular silo under uniform internal pressure around its circumference expand radially. Such a membrane has high horizontal membrane tensile stresses, but no horizontal bending moment. However if at any point the silo wall is attached to something that restrain its radial movement, the wall is dented and significant horizontal and vertical bending moments occur. These bending moment when their effect is added to the hoop tension and vertical compression could cause wall failure.

## 3.6 Live load

Pressure acting due to put away material are consider as a live load. Live load on stages, roof, and floors should be as required by applicable code. To determine the wall load flow condition must be check. Different procedure of determining design pressure must be used according to whether the flow is funnel flow, mass flow or some different type. Following three types of loads caused by a stored material on a structure are check for the designing of cylindrical Bin of silo.

Material and related Angle of Wall friction & Pressure ratio in Table 3.1:

Table 3.1: Angle of wall friction and pressure ratio.

| Material | Angle of wall friction | | Pressure ratio | |
|---|---|---|---|---|
| | While Filling | While Emptying | While Filling | While Emptying |
| Granular Materials with Mean particle diameter $\geq$ 0.2 mm | 0.75 | 0.6 | 0.5 | 1 |
| Powdery material with mean particle diameter less than 0.06 mm | 1 | 1 | 0.5 | 0.7 |
| Wheat Flour | 0.75 | 0.75 | 0.5 | 0.7 |

Here are some of the pressure acting on the silo as in Table 3.2 and stress distribution in Figure 3.1.

1. Horizontal load acting on the side walls due to horizontal pressure ($P_h$).
2. Vertical load due to vertical pressure ($P_v$)
3. Friction wall load acting on the cross sectional area of the bin filling

Table 3.2: Maximum pressure during filling and emptying.

| Sr No | Name of pressure | During filling | During emptying |
|---|---|---|---|
| 1 | Maximum $P_W$ | $WR$ | $WR$ |
| 2 | Maximum $P_h$ | $WR/\mu_f$ | $WR/\mu_f$ |
| 3 | Maximum $P_v$ | $WR/(\mu_f \lambda_f)$ | $WR/(\mu_f \lambda_f)$ |

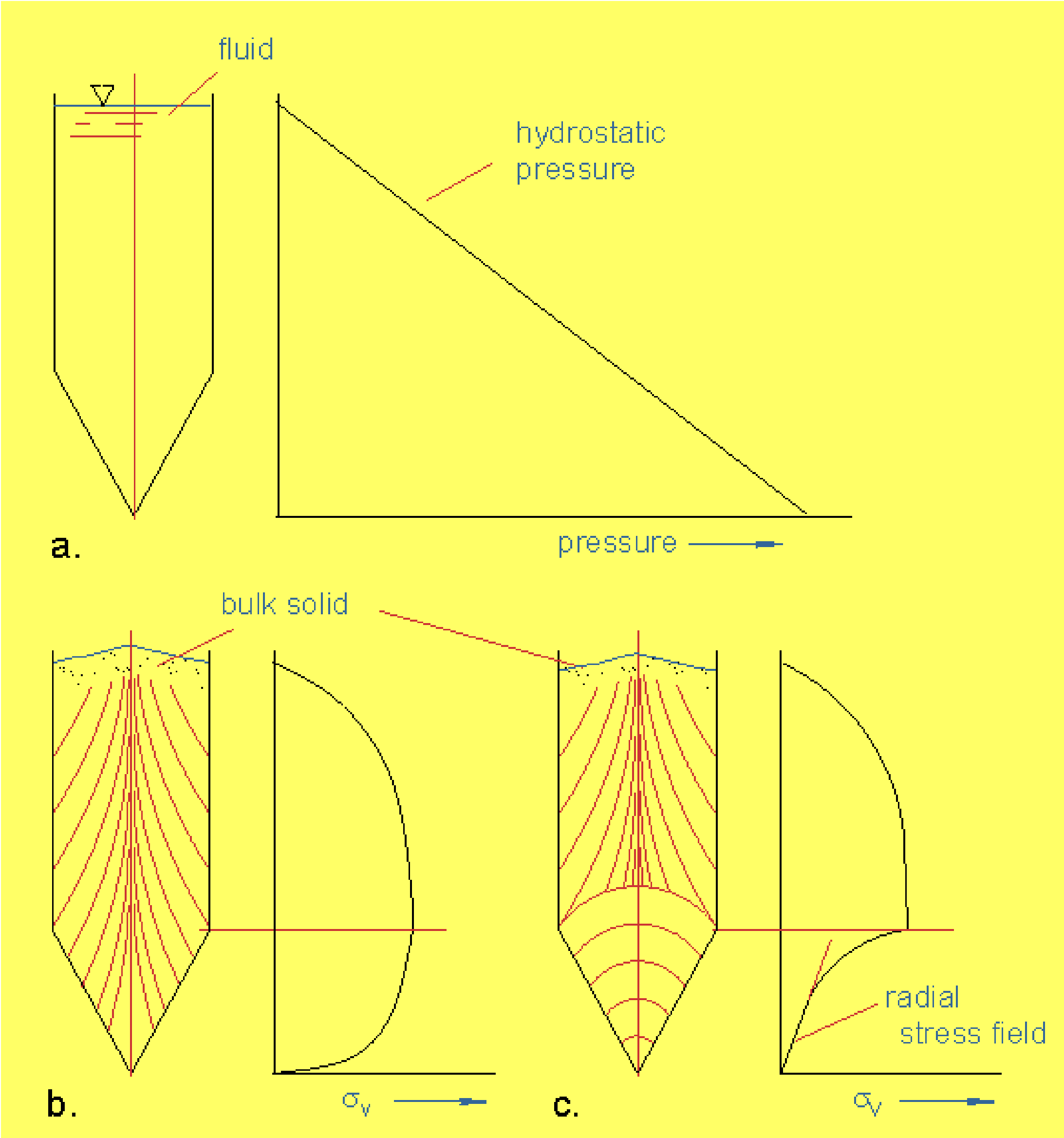


Figure 3.1: Stress Distribution.

# Chapter 4

# Design of Silo Components

## 4.1 Design input.

Capacity of silo =115$m^3$

Material to be stored = L.L.D.P.E. plastic pellet

Lower diameter of hopper $d_a$ =150 mm

Angle of internal wall friction ($\varnothing$) =28 degree

Angle of inclination of hopper = 60 degree

Bulk density of material ($\rho$) =650 $kg/m^3$

Filling eccentricity $e_f$=0 mm

Discharging eccentricity $e_0$ =0 mm

Height over ground $H_0$ =6000 mm

## 4.2 Cylindrical bin Design

Selection of height and diameter as per the required capacity.

First requirement for designing the cylindrical bin is to decide height and diameter as per required capacity of the silo. For the typical sizes and corresponding nominal capacity ($m^3$) as per the API standard the Table 4.1 is tabulated.

Table 4.1: Typical sizes and corresponding nominal capacity

| D(m) | Capacity/m ($m^3$) | Tank height in meter/No of course required | | | | |
|---|---|---|---|---|---|---|
| | | 4.8/2 | 7.2/3 | 9.6/4 | 12/5 | 14.4/6 |
| 3 | 7.07 | 34 | 51 | 68 | - | - |
| 4.5 | 15.9 | 76 | 115 | 153 | 191 | - |
| 6 | 28.3 | 136 | 204 | 272 | 339 | 407 |
| 7.5 | 44.2 | 212 | 318 | 424 | 530 | 636 |

$$C = 0.785 \times H \times D^2 \tag{4.1}$$

C=Capacity of tank in $m^3$

D=Diameter of tank in meter

H=Height of tank in meter

By trial and error method following parameters are obtained from Table the silo having 2400 mm Course height and 115 $m^3$ Capacity.

Diameter of silo =4500 mm

eight of cylindrical bin =7300 mm

Volume of cylindrical bin =115 m

## 4.3 Construction material

Mechanical property of the aluminum alloy material has been taken from the European code.Table 4.2 shows allowable stresses EN AW 5754 & EN AW 5083and respectively in Table 4.4 & Table 4.5 for material EN AW 5083. .

Table 4.2: Allowable stresses for EN AW 5754.

| EN AW 5754 | Tensile Stress | | Min. Allowable Compressive Stress to Ensure Stability | | Equivalent Stress | |
|---|---|---|---|---|---|---|
| | $\sigma_{zul,Z,LFT}$ | $\sigma_{zul,Z,LFT}$ | $\sigma_{zul,Z,LFHT}$ | $\sigma_{zul,Z,LFHT}$ | $\sigma_{zul,Z,LFHT}$ | $\sigma_{zul,Z,LFHT}$ |
| | $N/mm^2$ | $N/mm^2$ | $N/mm^2$ | $N/mm^2$ | $N/mm^2$ | $N/mm^2$ |
| At Ambient Temperature | 46.00 | 54.00 | 34.50 | 40.50 | 60.00 | 64.00 |
| At Operating Temperature | 46.00 | 54.00 | 34.50 | 40.50 | 60.00 | 64.00 |
| Weld Seams At Operating Temperature | 39.10 | 45.90 | 34.50 | 40.50 | - | - |

Table 4.3: Material property for EN AW 5754.

| | | |
|---|---|---|
| Material EN AW 5754[14] | | |
| Design temperature: | T=80$^\circ$ | Ct=1.00 |
| RP 0.2=80N/mm$^2$ | E=70N/mm$^2$ | $\mu_m$=0.75 |
| RP 0.2(T )=80N/mm$^2$ | E(T)=68N/mm$^2$ | E*(T)=53N/mm$^2$ |
| Safety factors: | LFH:Y=1.70 | LFHZ:Y=1.50 |

EN AW 5083

Table 4.4: Material property for EN AW 5083

| | | |
|---|---|---|
| Material EN AW 5083 | | |
| Design temperature: | T=80 $\circ$ | Ct=1.00 |
| $R_P$0.2=125N/mm$^2$ | E=70N/mm$^2$ | $\mu_m$=0.85 |
| $R_P$0.2(T )=125N/mm$^2$ | E(T)=68N/mm$^2$ | E*(T)=63N/mm$^2$ |
| Safety factors: | LFH:Y=1.70 | LFHZ:Y=1.50 |

Table 4.5: Allowable stresses for EN AW 5083

| EN AW5083 | Tensile Stress | | Min. Allowable Compressive Stress to Ensure Stability | | Equivalent Stress | |
|---|---|---|---|---|---|---|
| | $\sigma_{zul,Z,LFT}$ | $\sigma_{zul,Z,LFT}$ | $\sigma_{zul,Z,LFHT}$ | $\sigma_{zul,Z,LFHT}$ | $\sigma_{zul,Z,LFHT}$ | $\sigma_{zul,Z,LFHT}$ |
| | $N/mm^2$ | $N/mm^2$ | $N/mm^2$ | $N/mm^2$ | $N/mm^2$ | $N/mm^2$ |
| At Ambient Temperature | 74.00 | 84.00 | 62.90 | 71.40 | 93.80 | 100.00 |
| At Operating Temperature | 74.00 | 84.00 | 62.90 | 71.40 | 93.80 | 100.00 |
| Weld Seams At Operating Temperature | 62.90 | 71.40 | 34.50 | 40.50 | - | - |

## 4.4 Load on Cylindrical Bin.

1. Load on silo wall due to pressure acting by stored material during filling and discharging
2. Dead load due to weight of bin.
3. Live load
4. Wind load

### Load acting by stored material During Filling and Discharging on silo.

From Table 3.1 maximum pressure ratio during filling & emptying are 0.5 & 1 respectively.

Area $A = \pi/4 \times d^2 = 15.89 m^2$

Perimeter $U = 2 \times \pi \times r$= 14.13 m

Hydraulic mean radius $R = A/U$= 1.125 m

From angle of internal friction of stored material $\varnothing$ angle of wall friction during filling and discharged condition has been determined.

Filling Angle of wall friction $(\delta) = 0.75\varnothing = 21.00deg.$

Emptying Angle of wall friction $(\delta_e) = 0.6\varnothing = 16.80deg.$

Filling Coefficient of wall friction $(\mu_f) = tan(\mu_f) = 0.384$

Emptying Coefficient of wall friction $(\mu_e) = tan(\mu_e) = 0.302$

Pressure variation along bin depth:

$$Pi(z) = Pimax \times (1 - e^{-z/z_0}) \tag{4.2}$$

Where,

$Pw$ = wall pressure,

$Pi$= Horizontal pressure

$Pv$= Vertical pressure .

Here, Table 4.6 shows maximum pressure which has been calculated with help of table 3.2

During filling

$$Z_{0f} = R/(\mu_f \times \lambda_f) = 5.85m \tag{4.3}$$

During emptying

$$Z_{0e} = R/(\mu_e \times \lambda_e) = 3.725m \tag{4.4}$$

Pressure variation during filling & discharging conditions are shown in Table 4.5 &

Table 4.6 calculation in Figure 4.7 & Figure 4.8 respectively. Figure 4.1, 4.2 & 4.3 shows the variation of wall friction pressure, horizontal pressure & vertical pressure variation respectively.

Table 4.6: Maximum pressure calculation

| Sr. no | Name of pressure | During filling | During Emptying |
|---|---|---|---|
| 1 | Maximum $P_w$ | 3.93 | 3.93 |
| 2 | Maximum $P_h$ | 10.62 | 13.10 |
| 3 | Maximum $P_v$ | 19.65 | 13.10 |

Table 4.7: Pressure acting during filling condition

| depth (Z) meter | $Z/Z_{0f}$ | e$-^{Z/Z_{0f}}$ | X$_f$= $1-e^{-z/z_{0f}}$ | $P_w \times X_f$ $kN/m^2$ | $P_h \times X_f$ $kN/m^2$ | $P_v \times X_f$ $kN/m^2$ |
|---|---|---|---|---|---|---|
| 1 | 0.17094 | 0.842872 | 0.157128 | 0.617513 | 1.668699 | 3.087565 |
| 2 | 0.34188 | 0.710433 | 0.289567 | 1.137997 | 3.075199 | 5.689987 |
| 3 | 0.51281 | 0.598804 | 0.401196 | 1.576990 | 4.260699 | 7.883496 |
| 4 | 0.68371 | 0.504715 | 0.495285 | 1.946469 | 5.259923 | 9.732343 |
| 5 | 0.85471 | 0.42541 | 0.57459 | 2.258137 | 6.102141 | 11.29069 |
| 6 | 1.02561 | 0.358567 | 0.641433 | 2.520833 | 6.812023 | 12.60417 |
| 7 | 1.19651 | 0.302226 | 0.697774 | 2.742253 | 7.410363 | 13.71127 |
| 8 | 1.36751 | 0.254738 | 0.745262 | 2.928881 | 7.914687 | 14.64441 |
| 9 | 1.53842 | 0.214711 | 0.785289 | 3.086185 | 8.339767 | 15.43093 |
| 10 | 1.70942 | 0.180974 | 0.819026 | 3.218772 | 8.698056 | 16.09386 |

Table 4.8: Pressure acting during emptying condition

| Depth (Z) meter | $Z/Z_{0e}$ | e$-^{Z/Z_{0e}}$ | $X_e$=$1-e^{-Z/Z_{0e}}$ | $P_w \times X_e$ kN/ m$^2$ | $P_h \times X_e$ kN/ m$^2$ | $P_v \times X_e$ kN/ m$^2$ |
|---|---|---|---|---|---|---|
| 1 | 0.26845 | 0.76455 | 0.23544 | 0.925284 | 2.500386 | 4.62642 |
| 2 | 0.53691 | 0.58455 | 0.41545 | 1.632718 | 4.412078 | 8.16359 |
| 3 | 0.80536 | 0.44692 | 0.55307 | 2.173593 | 5.873679 | 10.86796 |
| 4 | 1.07382 | 0.34169 | 0.65830 | 2.587124 | 6.991158 | 12.93562 |
| 5 | 1.34228 | 0.26129 | 0.73875 | 2.903292 | 7.845537 | 14.51646 |
| 6 | 1.61073 | 0.19974 | 0.80026 | 3.145021 | 8.498760 | 15.72511 |
| 7 | 1.87919 | 0.15271 | 0.84728 | 3.329838 | 8.998187 | 16.64919 |
| 8 | 2.14765 | 0.11675 | 0.88324 | 3.471141 | 9.380029 | 17.35570 |
| 9 | 2.41610 | 0.08926 | 0.91073 | 3.579175 | 9.671969 | 17.89588 |
| 10 | 2.68456 | 0.06825 | 0.93174 | 3.661774 | 9.895175 | 18.30887 |

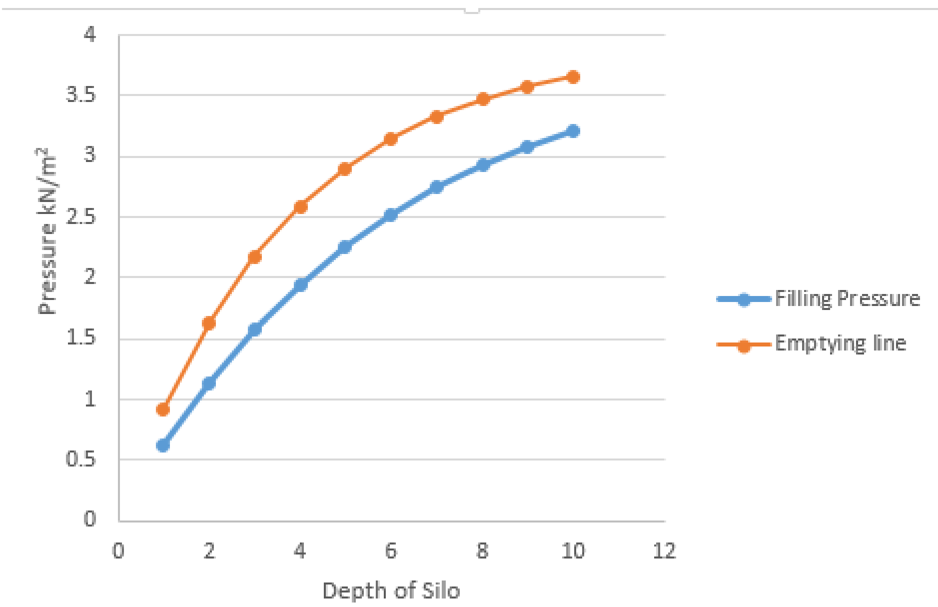


Figure 4.1: Wall frictional pressure during filling and emptying

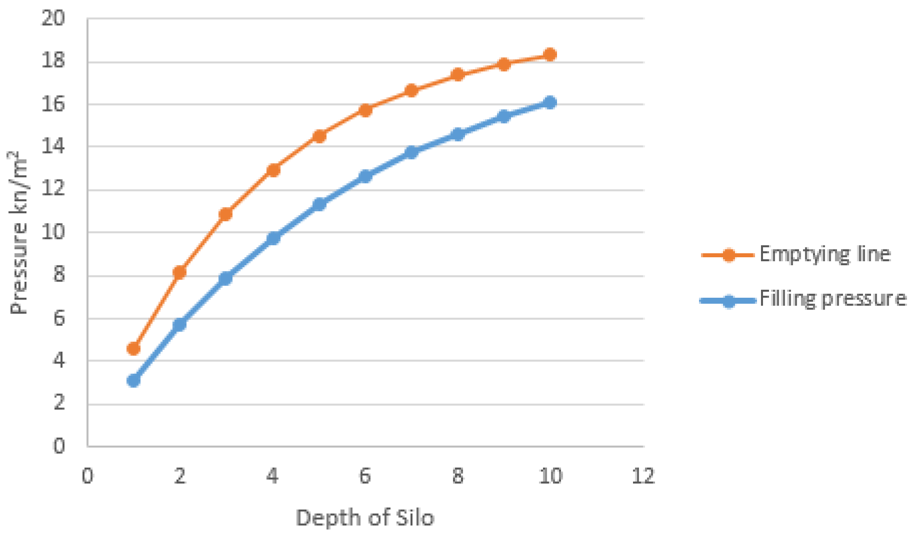


Figure 4.2: Vertical pressure during filling and emptying

## 4.5 Thickness calculation for cylindrical bin

Table 4.9 shows the calculation for the different shell section. Thickness calculation has been done by using below equations. Thickness of shell increasing from top to bottom as horizontal as well vertical pressure on shell wall increasing from top to bottom of silo.

$P_v$= Vertical pressure on shell wall

$P_h$= Horizontal pressure on shell wall

K = The ratio between horizontal and vertical pressure

$$P_v = w \times h_i \tag{4.5}$$

$$P_h = P_v \times K \times cos\alpha \tag{4.6}$$

$$t_{min} = \frac{p \times D}{2 \times S_d \times E + p} + C.A. \tag{4.7}$$

Table 4.9: Shell Thickness calculation

| No | $h_i$ | $P_v$ | $P_h$ | $t_d$ | $t_{min}$ | $t_{act}$ |
|---|---|---|---|---|---|---|
| 1 | 2500 | 0.016 | 0.014 | 3.937 | 5 | 5 |
| 2 | 5000 | 0.032 | 0.028 | 4.874 | 5 | 5 |
| 3 | 7500 | 0.048 | 0.042 | 5.811 | 5 | 6 |
| 4 | 10000 | 0.064 | 0.056 | 6.747 | 5 | 7 |
| 5 | 12500 | 0.080 | 0.070 | 7.683 | 5 | 8 |
| 6 | 15000 | 0.096 | 0.084 | 8.619 | 5 | 9 |
| 7 | 17500 | 0.112 | 0.098 | 9.555 | 5 | 10 |
| 8 | 20000 | 0.128 | 0.112 | 10.490 | 5 | 12 |

## 4.6 Dead load for cylindrical bin

Dead load includes weight of the silo it's self cylindrical bin, conical bottom, roof, skirt and additional dead loads on roof, railing, ladder load of the filter dead weight attachment etc. Calculation for the dead load of the cylindrical bin. Shows the dead load for various section of the cylindrical bin.

$$G = \rho \times V$$

$$G = \rho \times \pi \times D \times t \times h \tag{4.8}$$

Total dead load of the cylindrical bin is 19.7 kN

Table 4.10: Dead load for cylindrical bin

| Section | t(mm) | h(mm) | G(kN) |
|---|---|---|---|
| 1 | 5 | 2.5 | 6.35 |
| 2 | 5 | 2.5 | 6.35 |
| 3 | 6 | 2.5 | 6.9 |
| 4 | 7 | 2.5 | 7.35 |

## 4.7 Wind load

Wind pressure has been calculated according Indian standard "IS 875 (Part 3) - 1987" The basic wind speed ( $V_b$ ) for any site shall be obtained given in IS 875 and shall be modified to include the following effects to get design wind velocity at any height ($V_z$) for the chosen structure: It can be mathematically expressed as follows:

$$V_z = V_b * k_1 * k_2 * k_3 \tag{4.9}$$

Where

$V_b$ = design wind speed at any height z in m/s

$k_1$= probability factor (risk coefficient)

$k_2$= terrain, height and structure size factor and

$k_3$= topography factor.

The above mention three factor can be selected as per following guidelines

### Risk Coefficient ($k_1$)

The suggested life period is assumed in design and the corresponding factor $k_1$ can be selected for different class of structures for the purpose of design. Risk coefficient for different class of structure in different wind speed zone shall be selected from the IS 875 Part 3

### Terrain, height and structure size Factor ($k_2$)

Terrain - Selection of terrain categories shall be made with due regard to the effect of obstructions which constitute the ground surface roughness. The terrain category used in the design of a structure may vary depending on the direction of wind under consideration. Wherever sufficient meteorological information is available about the nature of wind direction, the orientation of any building or structure may be suitably planned. Terrain in which a specific structure stands shall be assessed as being one of the following terrain categories:

Category 1 - Exposed open terrain with few or no obstructions and in which the average height of any object surrounding the structure is less than 1.5 m.

Category 2 - Open terrain with well scattered obstructions having heights generally between I.5 to 10 m.

Category 3 - Terrain with numerous closely spaced obstructions having the size of building-structures up to 10 m in height with or without a few isolated tall structures.

Category 4 - Terrain with numerous large high closely spaced obstructions.

### Topography factor. ($k_3$)

The basic wind speed Vb takes account of the general level of site above sea level. This does not allow for local topographic features such as hills, valleys, cliffs, escarpments, or ridges which can significantly affect wind speed in their vicinity. The effect of topography is to accelerate wind near the summits of hills or crests of cliffs, escarpments or ridges and decelerate the wind in valleys or near the foot of cliffs, steep escarpments.

### Wind load calculation

Location of silo installation. X

Risk coefficient $k_1$=1.0

Local topographic factor $k_3 = 1.0$

Category of different terrains Category = “2”

Class of building or structure class := “B”

Wind pressure height variation factor $k_2$=[0.87,0.95,0.97,1.02,1.08]

Vz = [34.31,36.67,38.21,40.18,42.50] m/sec

Design wind pressure

$Pz = 0.6 \times Vz^2$

Pz =[0.708,0.807,0.878,0.967,1.084] kN/$m^2$

H=[10,20,30,50,100] m

### Moment due to wind on vertical wall Segments

Wind pressure Pz acting on silo and its magnitude vary with the height of the cylindrical bin Hz. Table 4.11 Shows moment ($m_{w,i,o}$) due to wind pressure of the cylindrical bin from base ring.

$$A_p = d \times h$$

$$H_{W,i,o} = P_{h,Wind} + A_p \tag{4.10}$$

$$m_{W,i,o} = H_{W,i} \times h_z \tag{4.11}$$

## 4.8 Self-supported conical roof design

Roof may be either self-supported or externally supported. It depends on the amount of external load, diameter of the silo and thickness of the roof plate. Usually for large silo diameter having thick roof plate required supporting structure. In this case it is not required as silo having six meter diameter. Self-supporting cone roofs shall conform to the following requirements.

D = nominal diameter of tank shell = 4.5 m

$\theta$= angle of cone elements with the horizontal = 15ř

t = nominal thickness of roof plates in mm.

As per IS 803 Clause 6.4.5 minimum thickness shall be greater than the value obtained from following formula.

$$t_{min} = D/(5 \times sin\theta) \tag{4.12}$$

$$t_{min} = 4.5/(5 \times sin15)$$

$$t_{min} = 3.84mm$$

$$t_{act} = 5.0mm$$

## 4.9 Designing of conical bottom

### 4.9.1 Thickness calculation for conical bottom

Conical bottom design has been done as per ASME SEC VIII DIVI. Thickness of section of the cone can be obtained based on maximum internal pressure.

Internal Pressure (P) =0.14 MPa

Diameter (D) =4500 mm

Half apex angle ($\alpha$) = 30ř

Material stress value(S) =60 MPa

Joint efficiency (E) =0.65

Required thickness,

$$t_c = \frac{p\times d}{2\times cos\alpha\times(S\times E - 0.6\times P} \tag{4.13}$$

Calculated conical bottom thickness for the section. Bottom thickness $t_c = 5$ mm

Table 4.11: Moment due to wind load on vertical segment

| Section | T | h(z) | h | D | $P_{h,Wind}$ | $A_p$ | $H_{W,i,o}$ | $m_{W,i,o}$ |
|---|---|---|---|---|---|---|---|---|
| 1 | 5 | 24.5 | 2.5 | 4.5 | 0.876 | 11.25 | 13.14 | 321.91 |
| 2 | 5 | 22 | 2.5 | 4.5 | 0.876 | 11.25 | 13.14 | 289.09 |
| 3 | 6 | 19.5 | 2.5 | 4.5 | 0.807 | 11.25 | 12.09 | 235.75 |
| 4 | 6 | 17 | 2.5 | 4.5 | 0.807 | 11.25 | 12.9 | 205.53 |

### 4.9.2 Filling & discharge pressure in hopper

Janssen silo pressure theory for vertical walls This theory is so critical to understanding many aspects of silos that the derivation is set out here. A tall silo with vertical walls, whose horizontal cross section can effectively take any shape. The equilibrium of forces on a slice of the solid with unit weight (or less formally bulk density) $\rho b$ at some depth z is shown, where the slice has height dz, plan area A and perimeter against the wall U. The stresses acting on it may vary across the horizontal surface above and below, and around the perimeter with the wall, so the mean values are used in this analysis. The mean vertical stress is q, the consequential mean horizontal pressure against the wall p and the frictional shear stress (termed frictional traction) on the wall $\tau$ . Vertical equilibrium of this slice of solid leads to

$$(q + dq)A + U\tau dz = qA + \rho bAdz \tag{4.14}$$

or

$$dqdzA + U\tau = \rho bA$$

The vertical stress q on the slice need not be uniform: the analysis considers only the mean value. Horizontal equilibrium of the slice requires some symmetry to exist in the wall pressures p, but they need not be constant around the perimeter (this becomes a serious issue later). Shear stresses on the top and bottom of the slice are assumed to integrate to a zero resultant on each face.

Two assumptions are next made (as used by Janssen): a The full wall friction is assumed to be developed against the wall at every point, so that the mean frictional shear $\tau$ is related to the mean normal pressure p on the wall through the wall friction coefficient $\mu$ as b

$$\tau = \mu p \tag{4.15}$$

The normal pressure p (mean value around the perimeter) is deemed to be related to the mean vertical stress q through a lateral pressure ratio K as

$p = Kq$

Inserting these into Equation

$$dz + UA\mu Kq = \rho_b$$

which may be solved to yield

$$q = q|z = 0 = 0 + \rho bA\mu U1 - e^{-zU/(AK\mu)}$$

If the mean vertical stress in the solid q is taken as zero at some reference height z = 0 (this condition is met at the centroid of the top pile of solids),

then q|z=0 = 0

and Equation (3.5) can be more neatly written as

$$q = q_0(1 - e^{-z/z_0})$$

where,$q_0 = \rho b z_0$ and $z_0 = 1/\mu K * A/U$

Here, $q_0$ represents the mean vertical stress in the solid that is reached asymptotically at great depth as shown in Figure 4.3. The length measure $z_0$ defines the rate at which the asymptote is approached and is commonly termed the Janssen reference depth. The origin of the vertical coordinate z (at the centroid of the top pile of solids) is called the equivalent surface.

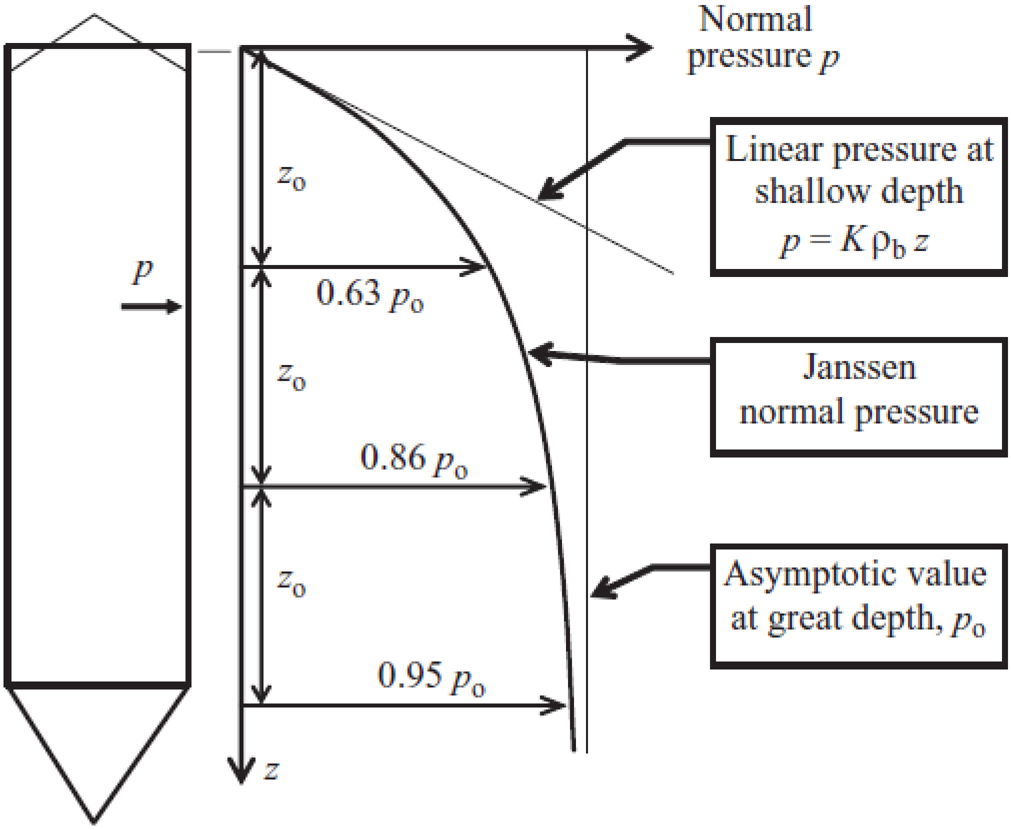


Figure 4.3: Silo and Hopper Design for strength

It is natural to transform into pressures normal to the wall p

$$p = p_0(1 - e^{-z/z_0}) \tag{4.16}$$

in which the asymptotic normal pressure at great depth is given by

$$p_0 = \rho b A \mu U = K \rho b z_0$$

The typical pattern of pressure defined by this equation . Since many silos have circular cross sections, it is useful to simplify the above equations to specialize them for a silo of radius

$$R.z_0 = R/2\mu K and p_0 = \rho b R/2\mu$$

The values of the wall friction coefficient $\mu$ and the lateral pressure ratio K may be measured in control tests on the particular solid being stored . A few deductions may be made from these equations. At great depth, the mean pressure p depends only on the radius R and the wall friction coefficient $\mu$, not on the depth below the surface. A smooth wall leads to higher pressures than a rough wall. The pressures all vary linearly with the solid bulk density $\rho b$, so this is a key parameter in any silo evaluation. The asymptotic value of pressure $p_0$ is actually more robust than the pressure distribution according to Janssen, because it does not need the assumption of a lateral pressure ratio. At great depth, conditions are stable, and neither the mean vertical stress q nor the mean wall pressure p changes. The equilibrium of a simple slice then simply equates the weight of the slice to the support given by wall friction, which becomes (adopting $\tau = \mu p$),

$$\mu p_0 U = \rho b A$$

or

$$p_0 = \rho b A/\mu U = \rho b R/2\mu$$

Thus, every theory that assumes that the wall friction is fully developed must reach the same asymptotic value of lateral pressure $p_0$ at great depth. This applies whether the silo is just filled or is being emptied. At shallow depths, the pressures vary linearly with depth and are approximated by

$$p = K\rho bz$$

which is the ‘earth pressure’ against a retaining wall. However, this theory does not take proper account of the surface profile in defining wall pressures near the surface, and this matters in squat silo geometries (see EN 1991-4 2007). The Janssen theory is the main descriptor of filling pressures in all standards.

## Pressures in hoppers

The Janssen theory describes pressures in a parallel-sided vessel as also shown in Figure 4.4 and distribution of discharge pressure in Figure 4.5 and in Table 4.12 pressure in conical bottom due to filling and graph is plotted in Figure 4.6 & Figure 4.7 for Normal pressre and Circumferential pressure respectively and consequently in Table 4.13 and in Figure 4.8 & 4.9 for Discharging condition. . The corresponding theory for a converging channel came much later, and is normally attributed to Walker (1964, 1966), though it was first derived by Dabrowski (1957) and was probably also found by Jenike and others in the late 1950s. The hopper height is H and the vertical coordinate is taken with its origin at the hopper apex, using coordinate x . The steepest line on the hopper is at angle $\beta$ to the vertical. For a conical or pyramidal hopper, the horizontal coordinate to the closest point on the wall is $r = xtan\beta$ and the area of a slice becomes

$$A = k_1 r^2 = k_1 xtan^2\beta$$

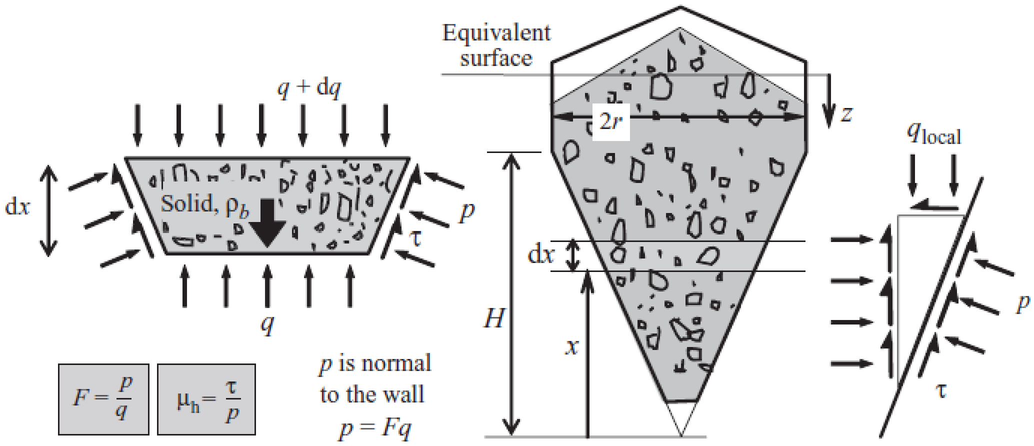


Figure 4.4: Bulk solid Handling

where $k_1 = \pi$ for a conical hopper and $k_1 = 4$ for a square hopper of half side r . The perimeter of the slice is given by

$$U = k^2 r = k^2 x\, tan\beta$$

where $k_2 = 2\pi$ for a conical hopper and $k_2 = 8$ for a square hopper of half side r . And further solving lead to the

$$n = 2[F + F\mu h cot\beta - 1] \tag{4.17}$$

which may be solved, considering the top boundary condition $q = q_t$ at $x = H$, to yield

$$q = q_t(\frac{x}{H})^n + \frac{\rho_b H}{(n-1)}\{(\frac{x}{H}) - (\frac{x}{H})^n\} \tag{4.18}$$

where $q_t$ is the mean vertical stress in the solid at the transition.

$$p = F\,[q_t\,(\frac{x}{H})^n + \frac{\rho_b H}{(n{-}1)}\,\{(\frac{x}{H}) - (\frac{x}{H})^n\}] \tag{4.19}$$

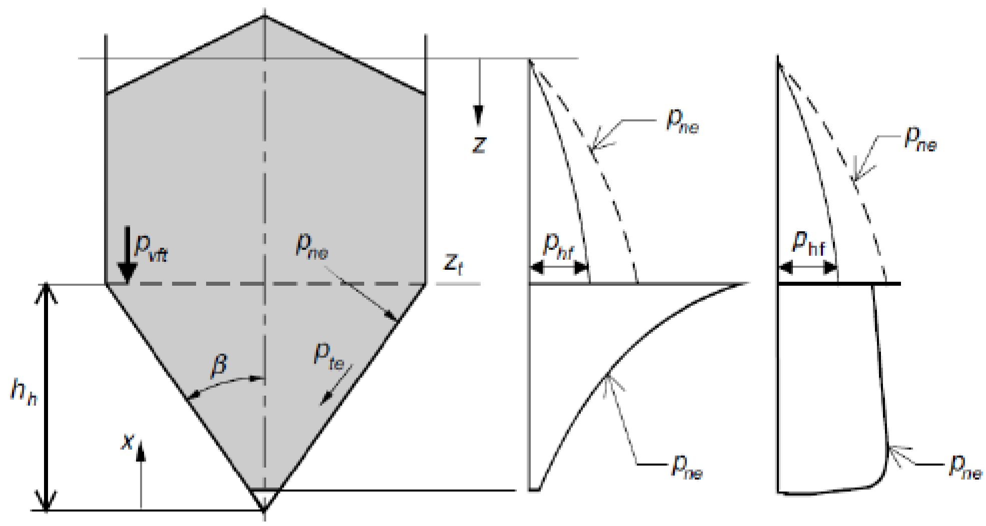


Figure 4.5: Distributions of discharge pressures in steep(1) and shallow(2) hoppers

Table 4.12: Pressure in conical bottom due to filling

| Sr. no | t | $H_h$ | x | x/$H_h$ | Diameter | $P_{vf}$ | $P_{nf}$ |
|---|---|---|---|---|---|---|---|
| 1 | 5 | 3.85 | 3.85 | 1 | 4500 | 17.721 | 10.633 |
| 2 | 5 | 3.85 | 3.5 | 0.9095 | 3914.285714 | 18.037 | 18.308 |
| 3 | 5 | 3.85 | 3 | 0.779220779 | 3328.57 | 18.056 | 18.056 |
| 4 | 5 | 3.85 | 2.5 | 0.649350649 | 2740 | 17.577 | 17.577 |
| 5 | 5 | 3.85 | 2 | 0.519480519 | 2155 | 16.52 | 16.52 |
| 6 | 5 | 3.85 | 1.5 | 0.38961039 | 1570 | 14.797 | 14.797 |
| 7 | 5 | 3.85 | 1 | 0.25974026 | 985 | 12.288 | 12.288 |
| 8 | 5 | 3.85 | 0.5 | 0.12987013 | 400 | 8.572 | 8.572 |

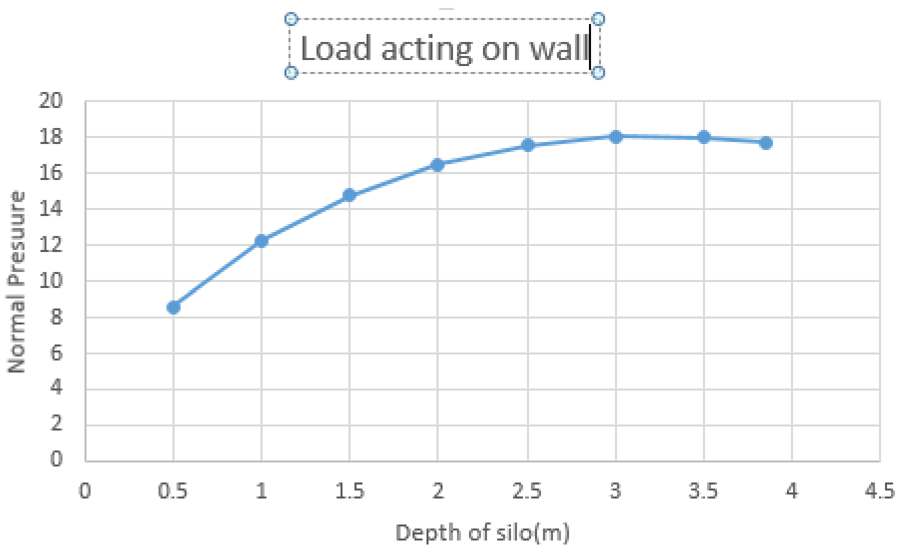


Figure 4.6: Wall pressure during filling

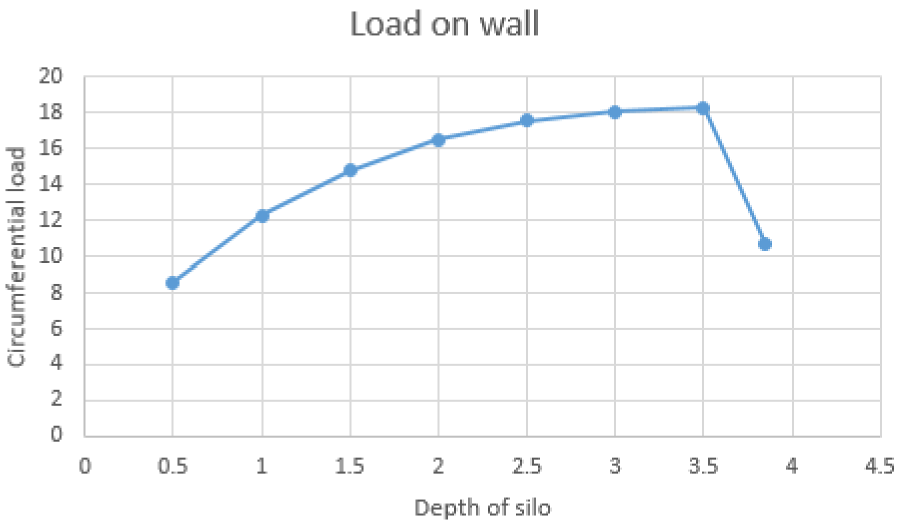


Figure 4.7: Wall pressure during filling

## Pressure in hopper during filling

Table 4.13: Pressure in conical bottom due to filling

| Sr. no | t | $H_h$ | x | $x/H_h$ | Diameter | $P_{vf}$ | $P_{nf}$ |
|---|---|---|---|---|---|---|---|
| 1 | 5 | 3.85 | 3.85 | 1 | 4500 | 17.727 | 10.665 |
| 2 | 5 | 3.85 | 3.5 | 0.9095 | 3914.285714 | 17.332 | 16.927 |
| 3 | 5 | 3.85 | 3 | 0.779220779 | 3328.57 | 15.892 | 15.555 |
| 4 | 5 | 3.85 | 2.5 | 0.649350649 | 2740 | 14.176 | 13.845 |
| 5 | 5 | 3.85 | 2 | 0.519480519 | 2155 | 12.164 | 11.880 |
| 6 | 5 | 3.85 | 1.5 | 0.38961039 | 1570 | 9.881 | 9.650 |
| 7 | 5 | 3.85 | 1 | 0.25974026 | 985 | 7.306 | 7.135 |
| 8 | 5 | 3.85 | 0.5 | 0.12987013 | 400 | 4.428 | 4.325 |

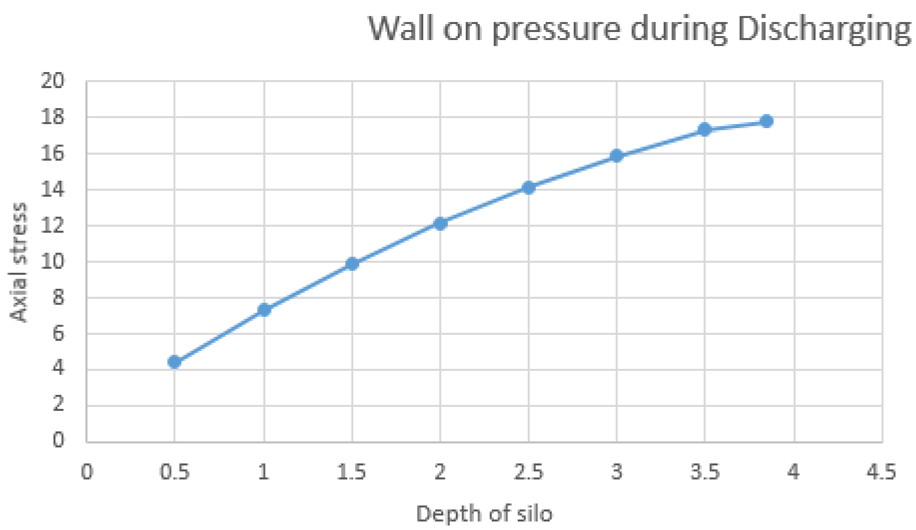


Figure 4.8: Wall pressure during discharging

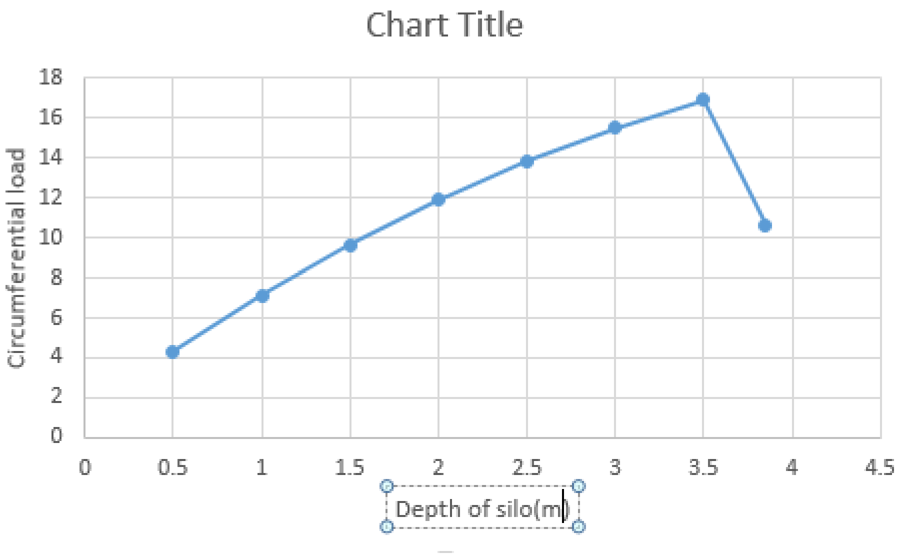


Figure 4.9: Wall pressure during discharging

# Chapter 5

# Stresses in Silo

Stresses are developed in silo due to filling and discharging of stored material, wind pressure, under pressure, over pressure or combination of this pressure. The stress in silo and the verification of the load bearing capability for the cylindrical silo chamber are explain in this section.

## 5.1 Stresses in cylindrical bin

Circumferential stress may be tensile or compressive in nature.

### 5.1.1 Circumferential Stress.

Tensile circumferential stress caused during discharge and over pressure condition while compressive circumferential stress induced at a time of wind and under pressure (Vacuum) condition.

#### Tensile circumferential stress.

The maximum tensile stress in circumferential direction is caused during discharge.Table 5.1 shows tensile Circumferential stress phi calculated during discharge ($P_{he}$) and over pressure. ($P_{hi}$).

$$P_h = P_{hi} + P_{he}$$

$$n_{phi} = P_h * Radius$$

$$\sigma = \frac{n_{phi}}{t}$$

Table 5.1: Tensile circumferential stress.

| Section | t mm | z m | $P_{he}$ $kN/m^2$ | $P_{hi}$ $kN/m^2$ | $P_h$ $kN/m^2$ | $n_{phi}$ $kN/m$ | $\sigma$ MPa |
|---|---|---|---|---|---|---|---|
| 1 | 5 | 2 | 3.07 | 3.2 | 2.50 | 7.50 | 1.50 |
| 2 | 5 | 3 | 4.27 | 3.2 | 4.40 | 13.20 | 2.64 |
| 3 | 5 | 4 | 5.25 | 3.2 | 5.80 | 17.40 | 3.48 |
| 4 | 5 | 5 | 6.10 | 3.2 | 6.90 | 20.97 | 4.19 |
| 5 | 5 | 6 | 6.82 | 3.2 | 7.85 | 23.52 | 4.70 |
| 6 | 5 | 7 | 7.40 | 3.2 | 8.46 | 24.47 | 5.09 |

Table 5.2: Compressive stress due to wind pressure

| Section | t mm | z m | $P_{hwind}$ kN/m$^2$ | $n_{phi}$ kN/m | $\sigma$ MPa |
|---|---|---|---|---|---|
| 1 | 5 | 2 | 0.876 | 2.628 | 0.5256 |
| 2 | 5 | 3 | 0.876 | 2.628 | 0.5256 |
| 3 | 5 | 4 | 0.876 | 2.628 | 0.5256 |
| 4 | 5 | 5 | 0.876 | 2.628 | 0.5256 |
| 5 | 5 | 6 | 0.876 | 2.628 | 0.5256 |

## Discharge Overpressure

One of the most frequent failure problems is the calculation of the overpressure coefficient, taking as a basis Janssen's formula for static pressure. After examining the theories and tests of more than 37 world specialists, it appeares that there is an envelope of lateral discharge pressure with a coefficient of 2.32 in relation to Janssen's pressure.

Janssen's formula is:

$$P_h = \frac{\delta.R}{tan\varphi} \tag{5.1}$$

$p_h$ =Horizontal pressure in $kg/m^2$

$\delta$ =Density of the ensiled material in $kg/m^3$

$R$ =Hydraulic radius , equal to the area/perimeter ratio of the straight section in meters

$\varphi$ =Angle of wall friction of the material

So, from the equation 4.20 we can calculate

$$P_h = \tfrac{903.5}{0.5317} = 1699.24kg/m^2$$

And now applying overpressure coefficient of 2.32, So

$$P_h = 3942.24kg/m^2$$

## Compressive stress due to wind pressure and discharge pressure.

Table 5.2 shows compressive stress due to wind pressure $P_{hwind}$ which is Calculated as per IS875 Part 3. Maximum value of stress due to wind pressure is at the top of silo & it is 0.5256 MPa.Table 5.3 shows circumferential compressive stress due to discharge pressure.

$$\sigma = \frac{n_{phi}}{t}$$

Table 5.3: Compressive Stress due to discharging

| Section | t mm | z m | $P_{hmin}.$ $kN/m^2$ | $n_{phi}$ $kN/m$ | $\sigma_{phi}$ $MPa$ |
|---|---|---|---|---|---|
| 1 | 5 | 2 | 0.5 | 1.125 | 0.1125 |
| 2 | 5 | 3 | 0.5 | 1.125 | 0.1125 |
| 3 | 5 | 4 | 0.5 | 1.125 | 0.1125 |
| 4 | 5 | 5 | 0.5 | 1.125 | 0.1125 |
| 5 | 5 | 6 | 0.5 | 1.125 | 0.1125 |
| 6 | 5 | 7 | 0.5 | 1.125 | 0.1125 |

### 5.1.2 Axial Stresses due to Various loads

Axial stress may be tensile or compressive in nature. Table 5.4 shows the axial stresses due to dead load, additional loads, roof load, wind load, discharges loads.This stresses used for finding out the tensile and compressive axial Stresses with the help of particular load case combination.

$$\sigma_{xg} = \frac{pd}{4t}$$

$$\sigma_{x,po} = \frac{pd}{4t}$$

Table 5.4: Axial stress due to various loads

| Axial Stress | | | Dead Load | | | Roof Loads | | | Discharge | |
|---|---|---|---|---|---|---|---|---|---|---|
| Sec. | t $mm$ | Z $m$ | W $kN$ | $A_c$ $mm^2$ | $\sigma_{xg}$ $\frac{kN}{mm^2}$ | W $kN$ | $A_c$ $mm^2$ | $\sigma_{xg}$ $\frac{kN}{mm^2}$ | Pressure $\frac{kN}{mm^2}$ | $\sigma_{x,po}$ $\frac{kN}{mm^2}$ |
| 1 | 5 | 7 | 10.33 | 141221 | 0.073 | 10.33 | 141221 | 0.073 | 2.5 | 0.5625 |
| 2 | 5 | 6 | 20.66 | 141221 | 0.146 | 10.33 | 141221 | 0.073 | 4.41 | 0.9923 |
| 3 | 5 | 5 | 30.99 | 141221 | 0.219 | 10.33 | 141221 | 0.073 | 5.87 | 1.3207 |
| 4 | 5 | 4 | 41.32 | 141221 | 0.292 | 10.33 | 141221 | 0.073 | 6.99 | 1.5727 |
| 5 | 5 | 3 | 61.72 | 104420 | 0.591 | 10.33 | 104420 | 0.099 | 7.84 | 1.7641 |
| 6 | 5 | 2 | 75.43 | 67580 | 0.111 | 10.33 | 67580 | 0.010 | 8.49 | 1.9102 |

## Tensile Stresses

Table 5.5 shows the tensile axial stress max which is computed by load case combination of dead load, wind load and over pressure.

$$\sigma = \frac{n_{phi}}{t}$$

Table 5.5: Tensile axial stress (Dead Load + Wind Load + Over pressure)

| Section | t mm | z (m) m | $n_{phi}$ | $\sigma$ MPa | Allowable Stress MPa | Utilization factor |
|---|---|---|---|---|---|---|
| 1 | 5 | 2 | 6 | 1.50 | 39.1 | 0.038363 |
| 2 | 5 | 3 | 9 | 2.64 | 39.1 | 0.067519 |
| 3 | 5 | 4 | 12 | 3.48 | 39.1 | 0.089003 |
| 4 | 5 | 5 | 15 | 4.20 | 39.1 | 0.107263 |
| 5 | 5 | 6 | 18 | 4.70 | 39.1 | 0.120307 |
| 6 | 5 | 7 | 21 | 5.10 | 39.1 | 0.130281 |

Table 5.6 shows the axial compressive stress with allowable stress and utilization factor

Table 5.6: Axial compressive stress

| Section | t mm | z m | $P_{hwind}$ | $\sigma_{hpi}$ MPa | Allowable Stress MPa | Utilization factor |
|---|---|---|---|---|---|---|
| 1 | 5 | 2 | 0.876 | 0.5256 | 40.5 | 0.012978 |
| 2 | 5 | 3 | 0.876 | 0.5256 | 40.5 | 0.012978 |
| 3 | 5 | 4 | 0.876 | 0.5256 | 40.5 | 0.012978 |
| 4 | 5 | 5 | 0.876 | 0.5256 | 40.5 | 0.012978 |
| 5 | 5 | 6 | 0.876 | 0.5256 | 40.5 | 0.012978 |
| 6 | 5 | 7 | 0.876 | 0.5256 | 40.5 | 0.012978 |

## 5.2 Stress verification

Stress verification has been done for the circumferential stresses,Axial stresses And Equivalent stresses. For all cases Utilization coefficient computed and proved that in all condition value of it is less than 1.

### 5.2.1 Tensile circumferential Stress verification

Table 5.7 shows tensile circumferential stress. It has been verified by taking discharge and over pressure load case combination. Value of the allowable circumferential tensile stress for material taken from mechanical property of the material EN AW 5754 and it is 39.10 N/mm$^2$ (allowable stress prevailing at the weld seams at operating temperature. Utilization coefficient has been found and maximum value of it is 0.138 which is less than 1 means stress due to load is not greater than allowable stress of the material.

Table 5.7: Verification of tensile circumferential Stress verication(Discharge +Overpressure)

| Section | Thickness mm | Resulting tensile force kN/m | Circumferential stress MPa | Allowable stress MPa | Utilization coefficient |
|---|---|---|---|---|---|
| 1 | 5 | 6 | 1.50 | 39.1 | 0.038363 |
| 2 | 5 | 9 | 2.64 | 39.1 | 0.067519 |
| 3 | 5 | 12 | 3.48 | 39.1 | 0.089003 |
| 4 | 5 | 15 | 4.20 | 39.1 | 0.107263 |
| 5 | 5 | 18 | 4.70 | 39.1 | 0.120307 |
| 6 | 5 | 21 | 5.10 | 39.1 | 0.130281 |

### 5.2.2 Compressive circumferential Stress

Table 5.8 shows compressive circumferential Stress. It has been verified by taking wind load and under pressure load case combination. Value of the allowable compressive circumferential stress for material taken from mechanical property of the material EN AW 5754 and it is 40.50 N/mm$^2$ (allowable stress prevailing at the weld seams at operating temperature. Utilization coefficient has been found and maximum value of it is 0.029 which is less than 1. Means stress due to loading is not greater than allowable stress of the material.

Table 5.8: Verification of Compressive circumferential Stress

| Section | Thickness mm | Resulting compressive force $kN/m$ | Circumferential stress MPa | Allowable stress MPa | Utilization coefficient |
|---|---|---|---|---|---|
| 1 | 5 | 2.628 | 0.5256 | 40.5 | 0.0129 |
| 2 | 5 | 2.628 | 0.5256 | 40.5 | 0.0129 |
| 3 | 5 | 2.628 | 0.5256 | 40.5 | 0.0129 |
| 4 | 5 | 2.628 | 0.5256 | 40.5 | 0.0129 |
| 5 | 5 | 2.628 | 0.5256 | 40.5 | 0.0129 |
| 6 | 5 | 2.628 | 0.5256 | 40.5 | 0.0129 |

### 5.2.3 Stresses in shell during filling

Figure 5.2 shows the maximum principal stress during filling of the material in the storage silo which is obtained with help of FE analysis & maximum value of this stress is 4.32 MPa. Table 5.10 shows the maximum principal stress during filling of the material,which is calculated theoretically & maximum value of this stress is 5.09 MPa. Figure 5.1 shows loading stage and Figure 5.3 shows Total deformation.

Table 5.9: Stresses in shell during filling

| Section | 1 | 2 | 3 | 4 | 5 | 6 |
|---|---|---|---|---|---|---|
| $\sigma_{phi}$ | 0.86 | 1.5 | 2.24 | 2.93 | 3.63 | 4.32 |
| $\sigma_x$ | 1.5 | 2.64 | 3.48 | 4.19 | 4.47 | 5.09 |

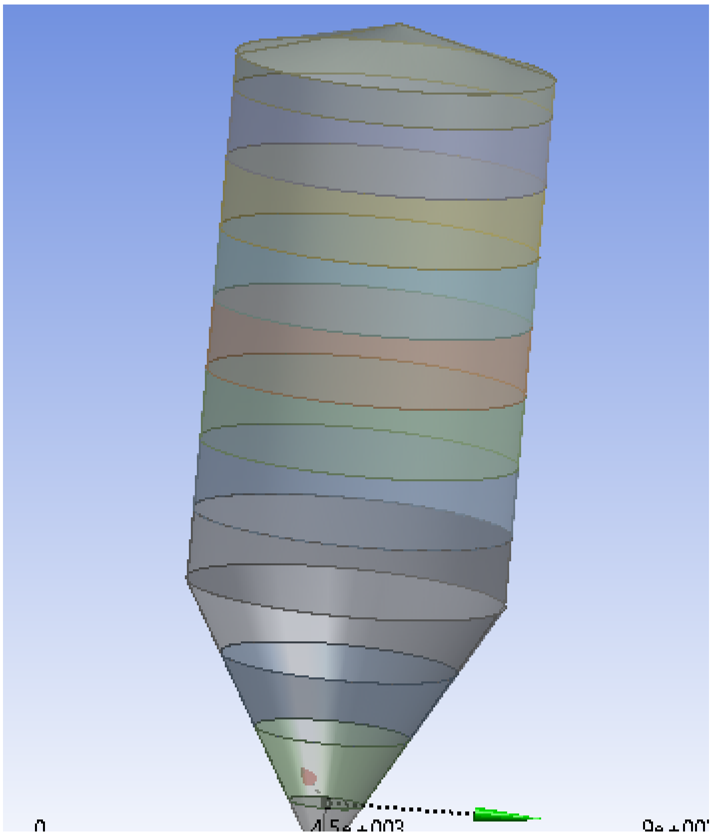

Figure 5.1: Loading stage

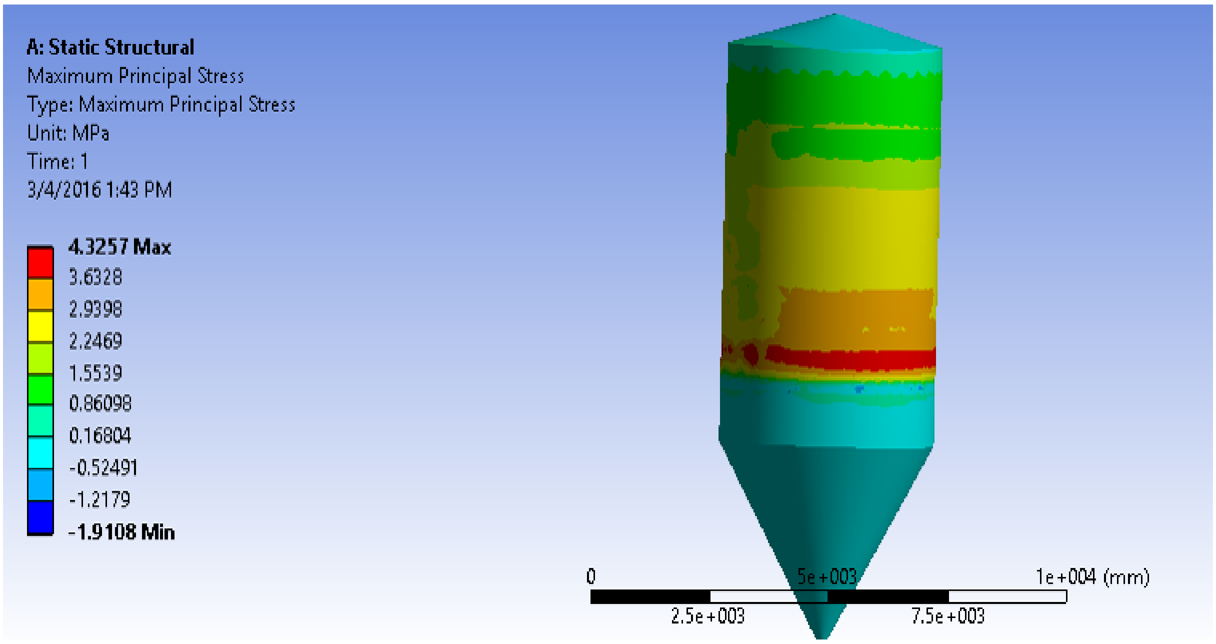


Figure 5.2: Maximum principal stress(MPa) in shell

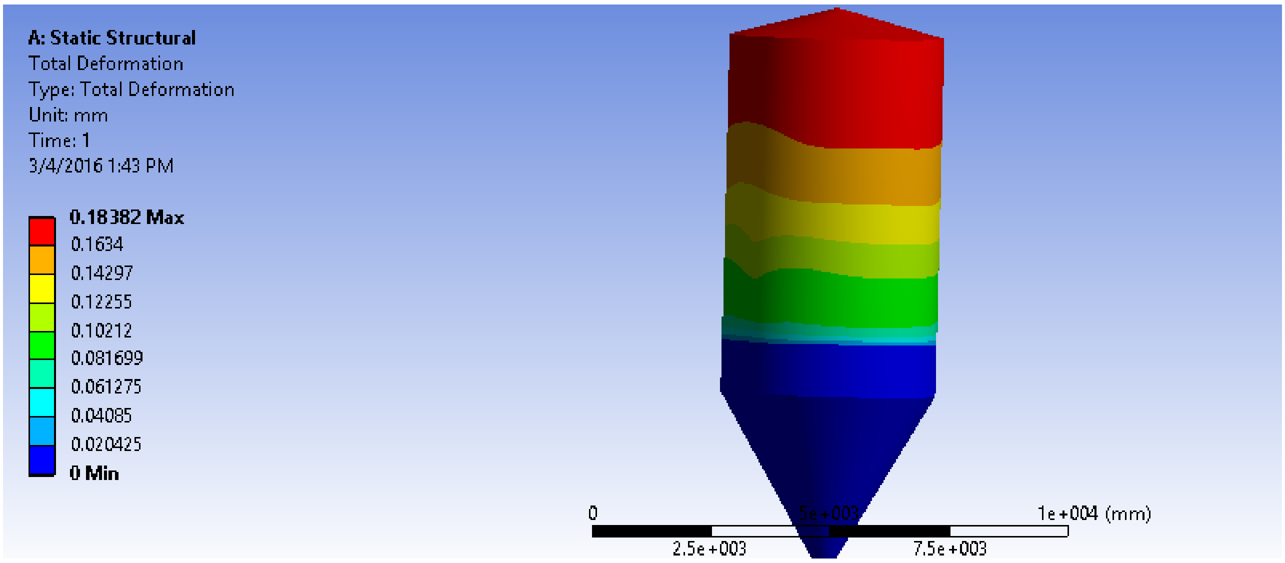


Figure 5.3: Total Deformation

## 5.3 Stresses in cone during filling and discharging

### 5.3.1 Stresses in cone during filling

Table 5.10 shows the maximum principal stress during filling of the material in the hopper, Table 5.11 shows the maximum principal stress during discharging of the material, which is calculated theoretically and maximum value of this stress is 6.98 MPa.

Table 5.10: Filling stress in conical bottom

| Sr. no | t mm | $H_h$ m | x m | $x/H_h$ | Diameter mm | $P_{vf}$ $kN/m^2$ | $P_{nf}$ $kN/m^2$ | $\sigma_{xf}$ $MPa$ | $\sigma_{Phi;fi}$ $MPa$ |
|---|---|---|---|---|---|---|---|---|---|
| 1 | 5 | 3.85 | 3.85 | 1 | 4500 | 17.721 | 10.63 | 4.78 | 2.39 |
| 2 | 5 | 3.85 | 3.5 | 0.9095 | 3914.28 | 18.03 | 18.30 | 8.23 | 4.11 |
| 3 | 5 | 3.85 | 3 | 0.7793 | 3328.57 | 18.05 | 18.05 | 8.12 | 4.06 |
| 4 | 5 | 3.85 | 2.5 | 0.6493 | 2740 | 17.57 | 17.57 | 7.90 | 3.95 |
| 5 | 5 | 3.85 | 2 | 0.5195 | 2155 | 16.52 | 16.52 | 7.43 | 3.717 |
| 6 | 5 | 3.85 | 1.5 | 0.3896 | 1570 | 14.79 | 14.79 | 6.65 | 3.32 |
| 7 | 5 | 3.85 | 1 | 0.2597 | 985 | 12.28 | 12.28 | 5.52 | 2.76 |
| 8 | 5 | 3.85 | 0.5 | 0.1298 | 400 | 8.57 | 8.57 | 3.85 | 1.92 |

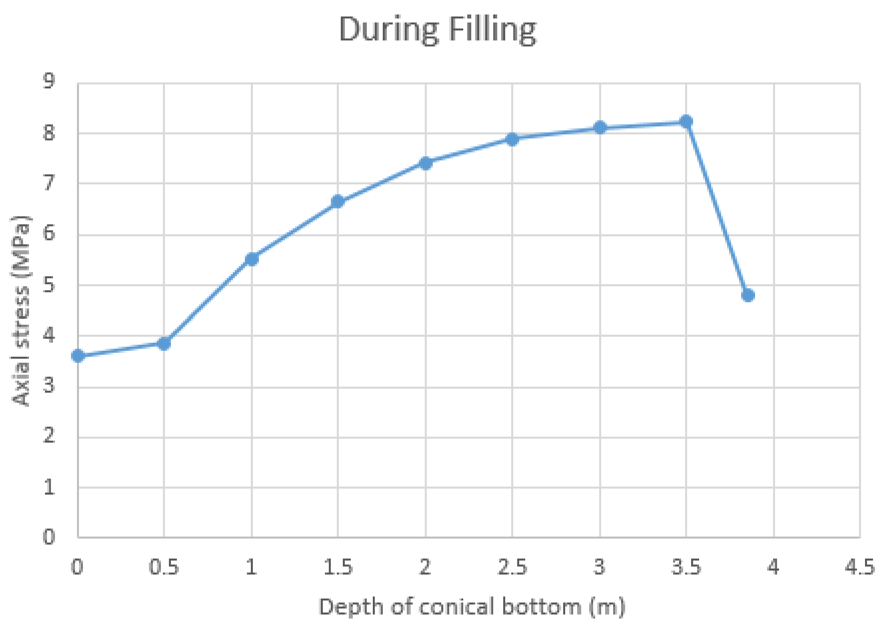


Figure 5.4: Axial stress during filling

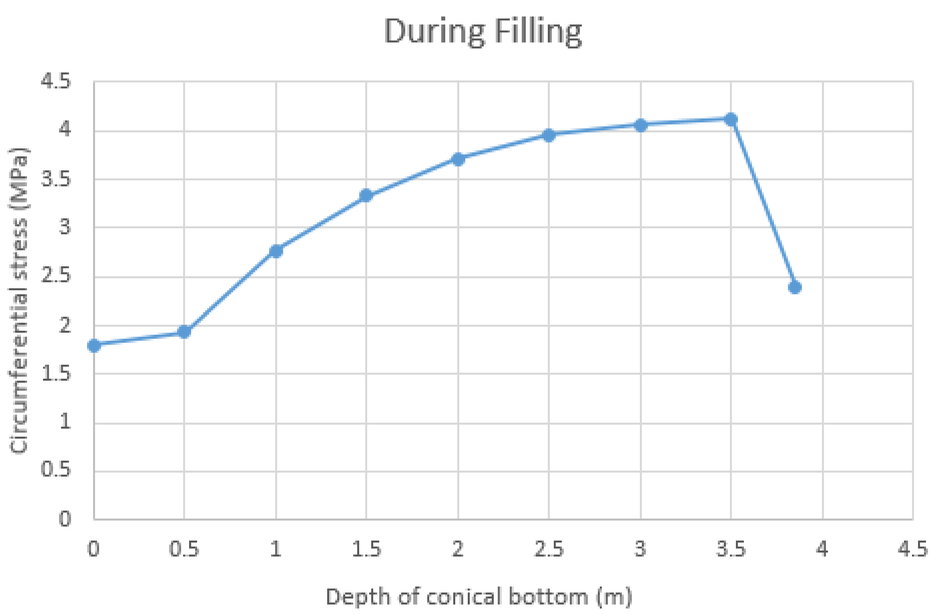


Figure 5.5: Circumferential stress during filling

### 5.3.2 Stresses in cone during discharging.

The maximum principal stress during discharging of the material, & maximum value of this stress is 6.98 MPa. Table 5.11 shows the maximum principal stress during discharging of the material, Figure 5.6 & Figure 5.7 shows axial stress and circumferential stress respectively which is calculated theoretically and maximum value of this stress is 6.98MPa.

Table 5.11: Discharging stress in conical bottom

| Sr. no | t $mm$ | $H_h$ $m$ | x $m$ | x/$H_h$ | Diameter $mm$ | $P_{vf}$ $kN/m^2$ | $P_{nf}$ $kN/m^2$ | $\sigma_{xf}$ $MPa$ | $\sigma_{Phi;fi}$ $MPa$ |
|---|---|---|---|---|---|---|---|---|---|
| 1 | 5 | 3.85 | 3.85 | 1 | 4500 | 17.78 | 10.66 | 4.79 | 2.41 |
| 2 | 5 | 3.85 | 3.5 | 0.9095 | 3914.28 | 17.73 | 16.92 | 7.61 | 3.80 |
| 3 | 5 | 3.85 | 3 | 0.7793 | 3328.57 | 15.91 | 15.52 | 6.98 | 3.49 |
| 4 | 5 | 3.85 | 2.5 | 0.6493 | 2740 | 14.17 | 13.84 | 6.22 | 3.114 |
| 5 | 5 | 3.85 | 2 | 0.5195 | 2155 | 12.16 | 11.88 | 5.34 | 2.673 |
| 6 | 5 | 3.85 | 1.5 | 0.3896 | 1570 | 9.881 | 9.65 | 4.34 | 2.17 |
| 7 | 5 | 3.85 | 1 | 0.2597 | 985 | 7.306 | 71.35 | 3.21 | 1.60 |
| 8 | 5 | 3.85 | 0.5 | 0.1298 | 400 | 4.438 | 4.335 | 1.94 | 0.973 |

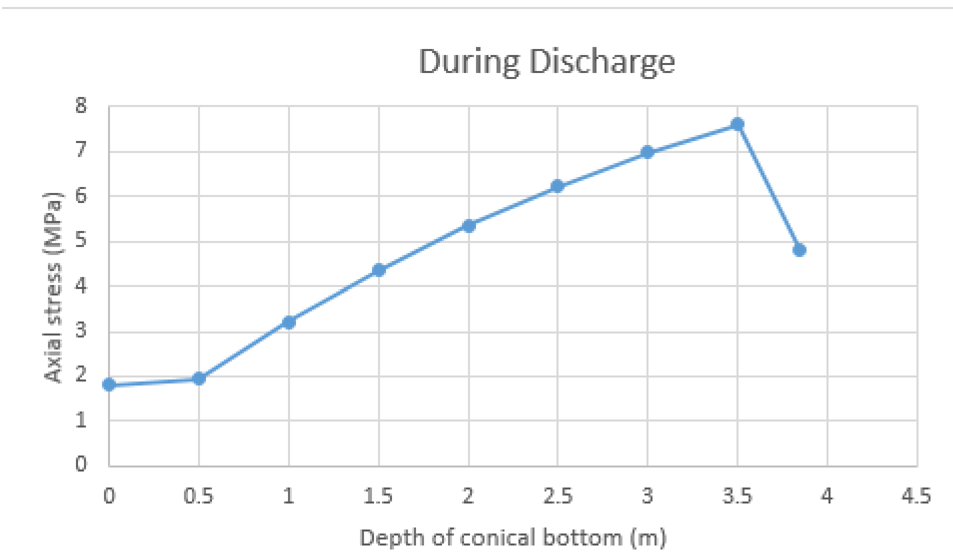


Figure 5.6: Axial stress during discharge

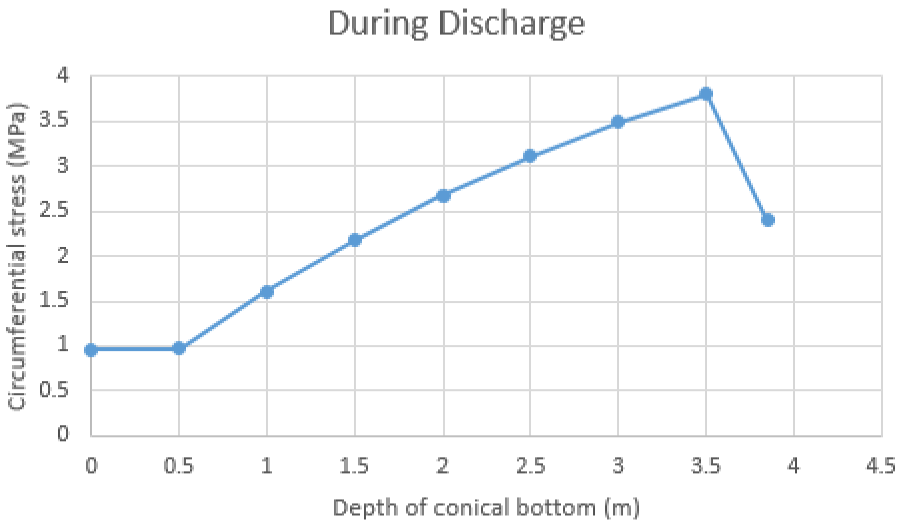


Figure 5.7: Circumferential stress during discharge

### 5.3.3 Calculation done by Silo Stress tool

SILO STRESS TOOL software is used to compare the stresses calculated as shown in Figure 5.8 & Figure 5.9 .

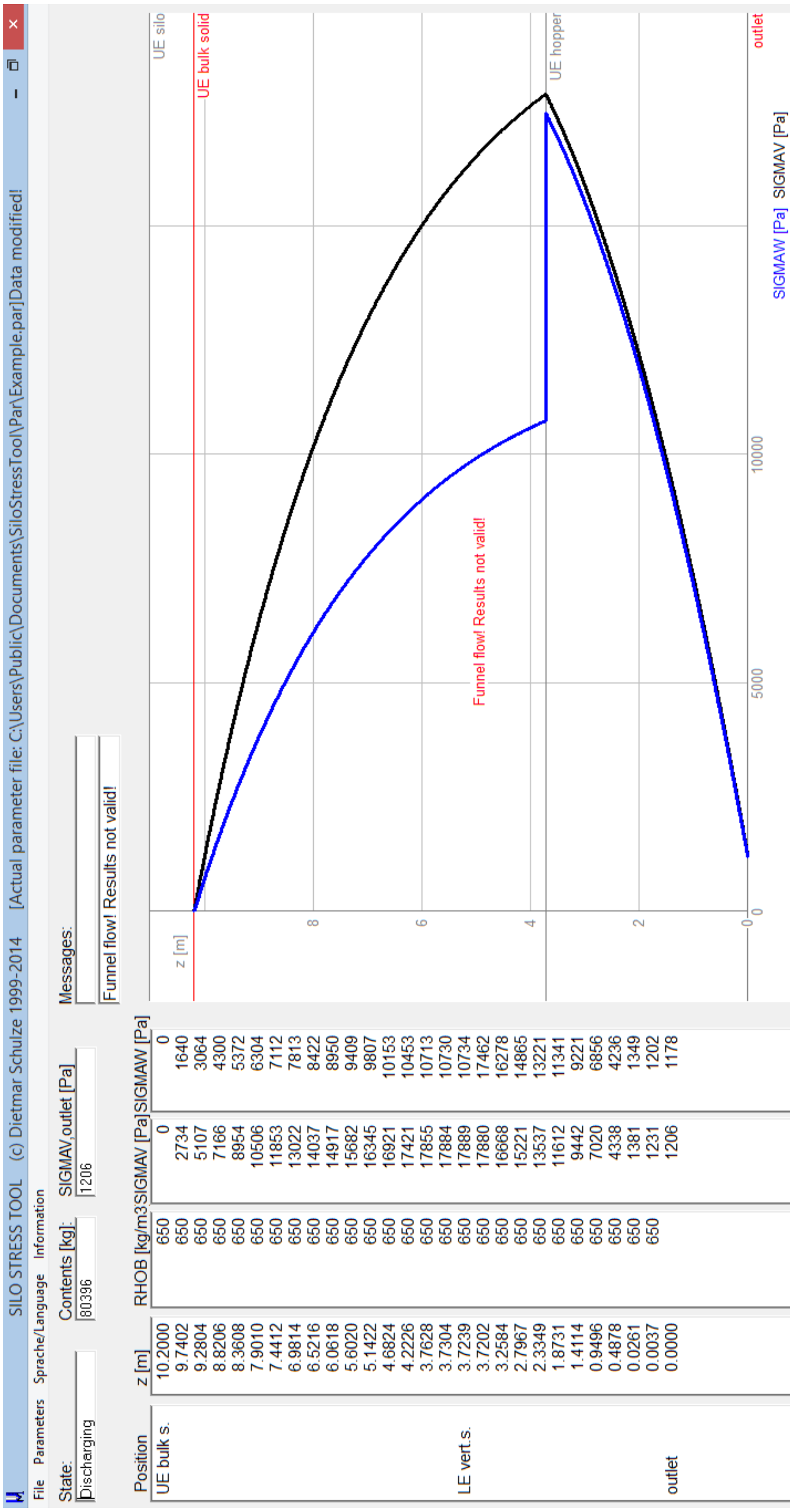


Figure 5.8: Stresses during discharging

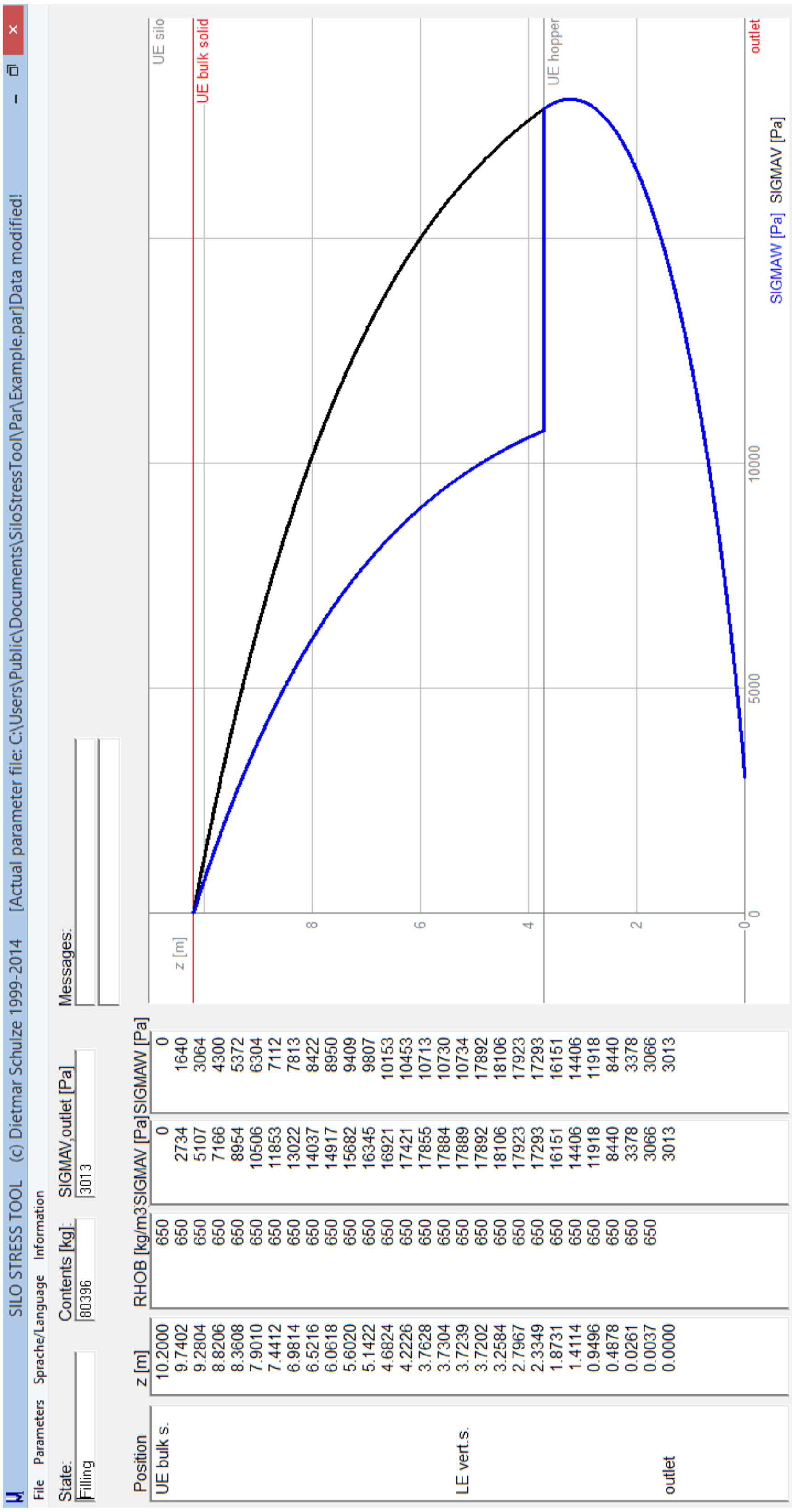


Figure 5.9: Stresses during feeling

# Chapter 6

# Design of transition junctions and supporting ring girders

## 6.1 Terminology

A ring whose purpose is only to provide resistance to radial components of forces from the hopper should be termed a ’transition ring’

A ring whose purpose is to provide redistribution of vertical forces between different Components.

The point of intersection between the middle surface of the hopper plate and the middle surface of the cylindrical shell wall at the transition junction, termed the ’joint centre’, should be used as the reference point in limit state verifications.

A silo with no identified ring at the transition has an effective ring formed from adjacent sheIl segments and should be termed a ’natural ring

An annular plate placed at the transition junction should be termed an ’annular plate ring’, see figure 7.1. A hot roIled steel section, used as a ring stiffener at the transition should be termed a ’rolled section ring’. A rolled steel section rolled around the silo circumference and used to support the shell beneath the transition should be termed a 'rolled ring girder.

An action built lip from steel plates with cylindrical and annular plate forms should be termed a 'fabricated ring girder'

## Modelling of the junction

In hand calculations, the junction should be represented by cylindrical and conical shell segments and annular plates only.

Where the silo is uniformly supported, the circumferential stresses in the annular plates of the junction may be assumed to be uniform in each plate.

Where the silo is supported on discrete supports or columns, the circumferential stresses in the junction plates should be taken to vary radially in each plate as a consequence of warping stresses.

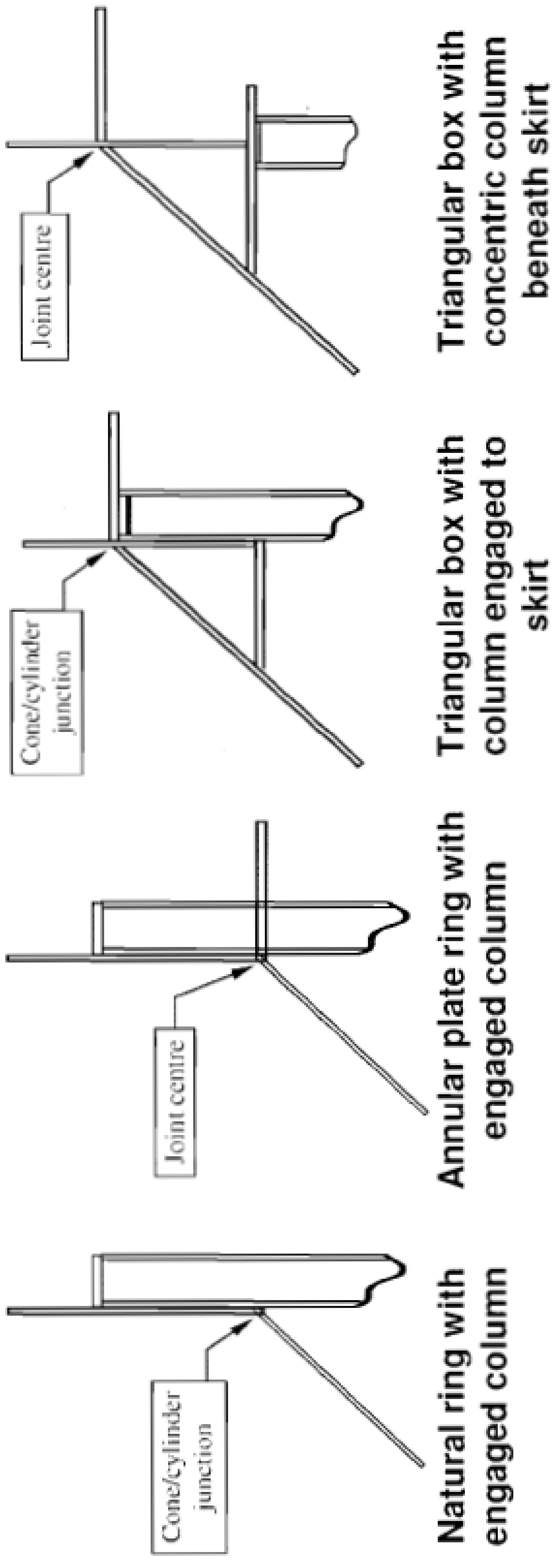


Figure 6.1: Ring forms

The equivalent thickness $t_{eqA}$ and $t_{eqB}$ of each group should be determined from:

$$t_{eqA} = \sqrt{\sum_{A} t^2} = 5mm \tag{6.1}$$

$$t_{eqB} = \sqrt{\sum_{B} t^2} = 7.81mm \tag{6.2}$$

The ratio $\alpha$ of the thinner to the thicker equivalent plate group should be determined from:

$$\alpha = \frac{(t_{eq})thinner}{(t_{eq})thicker} \tag{6.3}$$

with:

$$(t_{eq})thinner = min(t_{eqA}, t_{eqB}) = 5mm$$

$$(t_{eq})thicker = max(t_{eqA}, t_{eqB}) = 7.81mm$$

$$\alpha = \frac{(t_{eq})thinner}{(t_{eq})thicker} = \frac{5}{7.81} = 0.64$$

For the thinner of these two groups, the effective length of each shell segment should be determined from:

$$l_{e1=}0.778\sqrt{\frac{rt}{cos\beta}} \tag{6.4}$$

$$= 113.97 * 0.778$$

$$= 88.67mm$$

where $\beta$ is the angle between the shell centreline and the silo axis (cone apex half angle) for that plate. The effective cross-sectional area of each shell segment should be determined from:

$$A_{e1} = l_{e1}t \tag{6.5}$$

For the thicker of these two groups, the effective length of each shell segment should be determined from:

$$l_{e2} = 0.389[1 + 3\alpha^2 - 2\alpha^3]\sqrt{\frac{rt}{cos\beta}} \tag{6.6}$$

$$= 0.389 * 1.70 * 113.97$$

$$A_{e2} = l_{e2}$$

$$= 9.64$$

For this group, the effective cross-sectional area of each shell segment should be determined from:

$$A_{ep} = \frac{bt_p}{1 + 0.8\frac{b}{r}} \tag{6.7}$$

r which is the radius of the silo cylinder wall;

b which is the radial width of the annular plate ring;

$t_p$which is th thickness of the annular plate ring.

The total effective area Act of the ring in developing circumferential compression should be determined from:

$$A_{et} = A_{ep} + \sum A_{ei} \tag{6.8}$$

Where the junction consists only of a cylinder, skirt and hopper , the total effective area of the ring Act may be alternatively found from:

$$A_{et} = A_{ep} + 0.778\sqrt{r}\{t_c^{3/2} + \psi(\frac{t_h}{\sqrt{cos\beta}} + t_s^{3/2})\} \tag{6.9}$$

$$= (541.91 + 845.85)mm^2$$

$$= 1387.76mm^2$$

$$\psi = 0.5(1 + 3\alpha^2 - 2\alpha^3) \tag{6.10}$$

where,

$$\alpha = \frac{t_c}{\sqrt{t_s^2 + t_h^2}} = 0.64 \tag{6.11}$$

$$\psi = 1.70 * 0.5$$

$$\psi = 0.85$$

where in Figure 7.2:

r which is the radius silo;

$t_c$is the cylinder thickness;

$t_s$is the skirt thickness;

$t_h$ is the hopper thickness;

$A_{ep}$ is the annular plate ring's effective area;

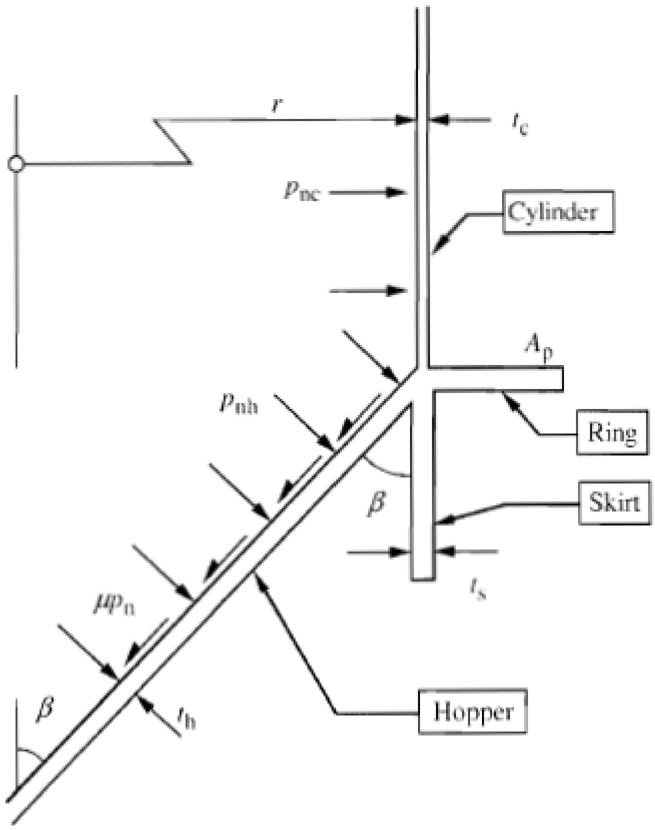


Figure 6.2: Notation for simple annular transition

The design value of the effective circumferential compressive force $N_{\theta Ed}$. developed in the junction should be determined from as in Figure 7.3;

$$N_{\theta Ed} = n_{\phi h,Ed} r sin\beta - p_{nc} r l_{ec} - p_{nh}(cos\beta - \mu sin\beta) r l_{eh} \tag{6.12}$$

$$= 15,890N$$

$n_{\phi h,Ed}$ is the design value of the meridional tension per unit circumference at the top of the hopper.

$p_{nc}$ which is the mean local pressure on the effective length of the cylinder segment

$p_{nh}$which is the mean pressure on the effective length of the hopper segment

$\mu$which is the hopper friction coefficient.

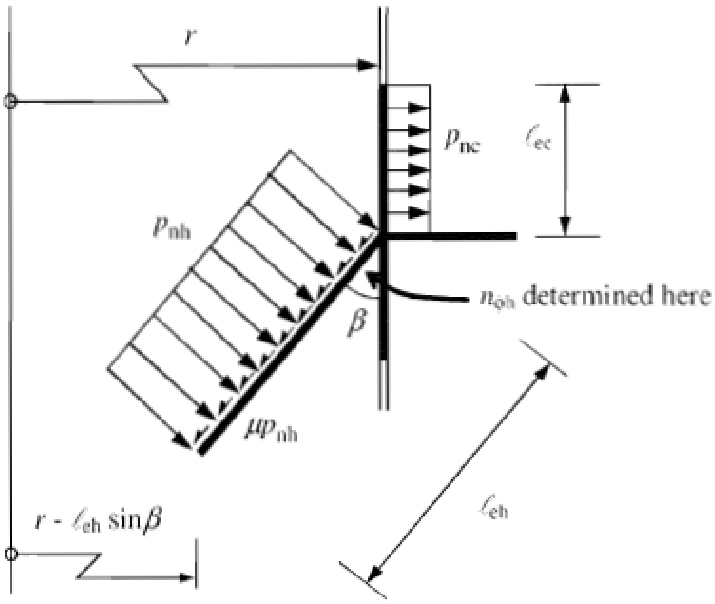


Figure 6.3: Local pressures and membrane stress resultant loadings on the transition ring

The maximum design compressive stress $\sigma_{u\theta,Ed}$ for the uniformly supported junction should be determined from:

$$\sigma_{u\theta,Ed} = \frac{N_{\theta,Ed}}{\eta A_{et}} \tag{6.13}$$

where,

$$\eta = 1 + 0.3\frac{b}{r} = 1.015 \tag{6.14}$$

$$\sigma_{u\theta,Ed} = 11.28MPa$$

# Chapter 7

# Conclusion & Future Work

## Conclusion

Designing of the silo components have been done using applicable codes and standards. Design load and pressure calculation has been done for cylindrical bin and conical hopper. Verification of circumferential, axial and equivalent stresses have been carried out considering dead load, live load, wind load and load due to filling and discharging pressure of the bulk material. Stresses in cylindrical bin and hopper have been obtained with help of FE analysis for pressure variation during filling and discharging condition and same has been compared with theoretical calculation. Also, Critical phase in silo is transition phase where cylindrical shell meets conical hopper which is vulnerable so that proper design of supporting ring girder which can prevent the failure. Which become necessary when the safety is much reliable on that phase.

## Future Work

FEA Analysis of the transition phase cone be done so that it can such that it also verify the mathematical model.

Variation of hopper pressure can be checked by replacing concentric hopper with eccentric hopper.

Optimization of shell thickness can be done by providing stiffeners on storage silo wall .

# References


[1] P. Vidal,E. Gallego,M. Guaita,F. Ayuga.,“Finite element analysis under different boundary conditions of the filling of cylindrical steel silos having an eccentric hopper Journal of Constructional Steel ”,Research 64 (2008) 480-492

[2] D. Briassoulis ,“Finite element analysis of a cylindrical silo shell under unsymmetrical pressure distributions Computers and Structures ”,78 (2000) 271-281.

[3] F.ayuga,P.agudo,E.gallego,A.ramirez “New steps towards the knowledge of silos behaviour ”, Int. Agrophysics, 2005, 19, 7-17.

[4] API650,“Appendix-A Table A-3a Typical sizes and corresponding capacity for 2400 mm course silo ”, Thin-Walled Structures 42 (2004) 1519-154.

[5] Dr.John W.Carson,“Silo Failures:Case histories and lessons learned ”

[6] Juana,J.M. Morana, M.I. Guerraa, A. Coutoa, F. Ayugab, P.J. Aguado ,“Aguado Establishing stress state of cylindrical metal silos using finite element method: Comparison with ENV 1993. ”, Thin-Walled Structures 44 (2006) 1192-1200.

[7] C.Y. Song, “Effect of patch loads on structural behaviour of circlar flat bottom steel silo”, Thin-Walled Structures 42 (2004) 1519-154.

[8] FuatTinis,Fatih Bazman,“Stiffening of thin cylindrical silo shell against buckling loads. ”, Industrial plant manufacturing and erection corp,06791,turky-2006.

[9] Y. Zhao, J.G. Teng, “Buckling experiments on steel silo transition junctions II: Finite element modeling ”, Journal of Constructional Steel Research 60 (2004) 1803-1823

[10] Y.Zhao, J.G.Teng,“Buckling experiments on steel silo transition junctions I: Experimental results”, Journal of Constructional Steel,Research 60 (2004) 1783-1801.

[11] Moss, Dennis R,“Pressure vessel design manual: illustrated procedures for solving major pressure vessel design problems ”, Thin-Walled Structures 42 (2004) 1519- 154

[12] DIN 1055 Part 6, “Design loads for building: Loads on silo bin”, 2005-03

[13] IS 875 Part 3, “Code of practice for design loads (other than earthquake) for building and structures. ”, 1987

[14] DIN 18800 part 4,“Analysis of safety against buckling of shell. ”, November 1990

[15] DIN EN 1991-4,“Eurocode 1: Actions on structures Part 4: Silos and tanks. ”,December 2006

[16] DIN EN 1993-4-1,“Eurocode 3: Design of steel structures Part 4-1: Silos. ”, December 2010

[17] DIN EN 1993-1-6, “Eurocode3: Design of steel structures Part 1-6: Strength and stability of shell structures ” , December 2010.

[18] B.C.Bhattacharyya, “Introduction to chemical equipment design, Mechanical aspects ” , CBS Publishers and Distributors (First edition:1985)

[19] IS 9178- 1980, “for Design of Steel bins for storage of bulk materials”, art 3 Bins design for mass flow and funnel flow”

[20] EN 1993-4-1 (2007) (English): Eurocode 3: Design of steel structures - Part 4-1: Silos [Authority: The European Union Per Regulation 305/2011, Directive 98/34/EC, Directive 2004/18/EC]